Supplementary material

The Role of Bridge for Single-Ion Magnet Behaviour: Reinvestigation of Cobalt(II) Succinate and Fumarate Coordination Polymers with Nicotinamide

Marek Brezovan[1], Jana Juráková[2], Ján Moncol[1], Ľubor Dlháň[1], Maria Korabik[3], Ivan Šalitroš[1,2,4], Ján Pavlik[1,*], Peter Segľa[1]

[1]Faculty of Chemical and Food Technology, Slovak University of Technology, Radlinského 9, 812 37, Bratislava, Slovakia
jan.pavlik@stuba.sk

[2]Central European Institute of Technology, Brno University of Technology, Purkyňova 123, 61200 Brno, Czech Republic

[3]Faculty of Chemistry, University of Wrocław, F. Joliot -Curie 14, 50-383 Wrocław, Poland

[4]Faculty of Science, Palacký University, 17. listopadu 12, 771 46 Olomouc, Czech Republic

Contents

S1 Crystallographic Characterization

Table S1 Crystallographic data for compounds **I** and **II**

	I	**II**
Chemical formula	$C_{16}H_{24}CoN_4O_{10}$	$C_{16}H_{18}CoN_4O_8$
M_r	491.323	453.277
Crystal system	Triclinic	Triclinic
Space group	$P\bar{1}$	$P\bar{1}$
T / K	100(1)	100(1)
a / Å	7.4478(2)	7.2175(2)
b / Å	7.8226(3)	7.5419(3)
c / Å	9.7729(3)	9.0156(3)
α / °	66.853(3)	109.677(3)
β / °	69.244(3)	103.138(3)
γ / °	76.561(3)	97.449(3)
V / Å^3	486.69(3)	438.48(3)
Z	1	1
λ (Cu–$K\alpha$ / Å	1.54186	1.54186
μ / mm^{-1}	7.52	8.205
Crystal size / mm	0.28 × 0.22 × 0.15	0.15 × 0.09 × 0.06
ρ_{calc} / g.cm^{-3}	1.676	1.717
S	1.060	1.145
R_1 [$I > 2\sigma(I)$]	0.0214	0.0196
wR_2 [all data]	0.0506	0.0448
$\Delta\rangle_{max}$, $\Delta\rangle_{min}$ / e Å^{-3}	0.25, –0.29	0.17, –0.32
CCDC	1976280	2105647

Table S2 Selected geometric parameters (Å) for **I** and **II**

I		II	
Co1–O1	2.0931(9)	Co1–O1	2.0683(8)
Co1–O1^{i}	2.0931(9)	Co1–O1^{ii}	2.0683(8)
Co1–N1	2.1672(12)	Co1–N1	2.1689(10)
Co1–N1^{i}	2.1672(12)	Co1–N1^{ii}	2.1689(10)
Co1–O1W	2.1090(10)	Co1–O1W	2.0924(9)
Co1–O1W^{i}	2.1090(10)	Co1–O1W^{ii}	2.0924(9)

Symmetry codes: (i) 1–x, 1–y, 2–z; (ii) 1–x, 1–y, –z

Table S3 Symmetry measure parameters obtained from SHAPE structural analysis and distortion parameters Σ calculated for coordination polyhedra **I** and **II**: hexagon (D_{6h}); pentagonal pyramid (C_{5v}); octahedron (O_h); trigonal prism (D_{3h}); Johnson pentagonal pyramid (C_{5v}); $\boldsymbol{\Sigma} = \sum_1^{12} |\varphi_i - 90|$; where φ_i presents *cis* angle in hexacoordinated polyhedron

	S(D_{6h})	S(C_{5v})	S(O_h)	S(D_{3h})	S(C_{5v})	$\boldsymbol{\Sigma}$ / ^{o}
Complex **I**	30.489	28.886	**0.198**	16.142	32.102	30
Complex **II**	29.212	28.243	**0.306**	16.069	31.322	43

Table S4 Parameters of H-bonds

	***d*(H···A)/Å**	***d*(D···A)/Å**	**D–H···A/°**
I at 100 K (HAR model)			
O1W–H1WA···O2W (1–x, 2–y, 2–z)	1.80(2)	2.758(1)	175(2)
O1W–H1WB···O2 (1+x, y, z)	2.03(2)	2.857(1)	152(2)
O2W–H2WA···O1	1.84(3)	2.794(1)	173(2)
O2W–H2WB···O3 (x, 1+y, z)	1.90(2)	2.834(1)	170(2)
N2–H2A···O3 (2–x, –y, 1–z)	1.97(2)	2.943(1)	160(2)
N2–H2B···O2 (1+x, y, –1+z)	2.10(2)	3.046(1)	169(2)
C3–H3···O2 (1+x, y, –1+z)	2.40(2)	3.357(1)	150(2)
II at 100 K (HAR model)			
O1W–H1WA···O3 (x,–1+y, z)	1.90(2)	2.822(1)	166(2)
O1W–H1WB···O2 (1+x, y, z)	1.82(2)	2.758(1)	167(2)
N2–H2A···O3 (2–x,3 –y, 1–z)	1.95(2)	2.972(1)	171(2)
N2–H2B···O2 (1+x, 1+y, 1+z)	1.92(2)	2.901(1)	170(2)
C3–H3···O2 (1+x, 1+y, 1+z)	2.19(2)	3.232(1)	161(2)

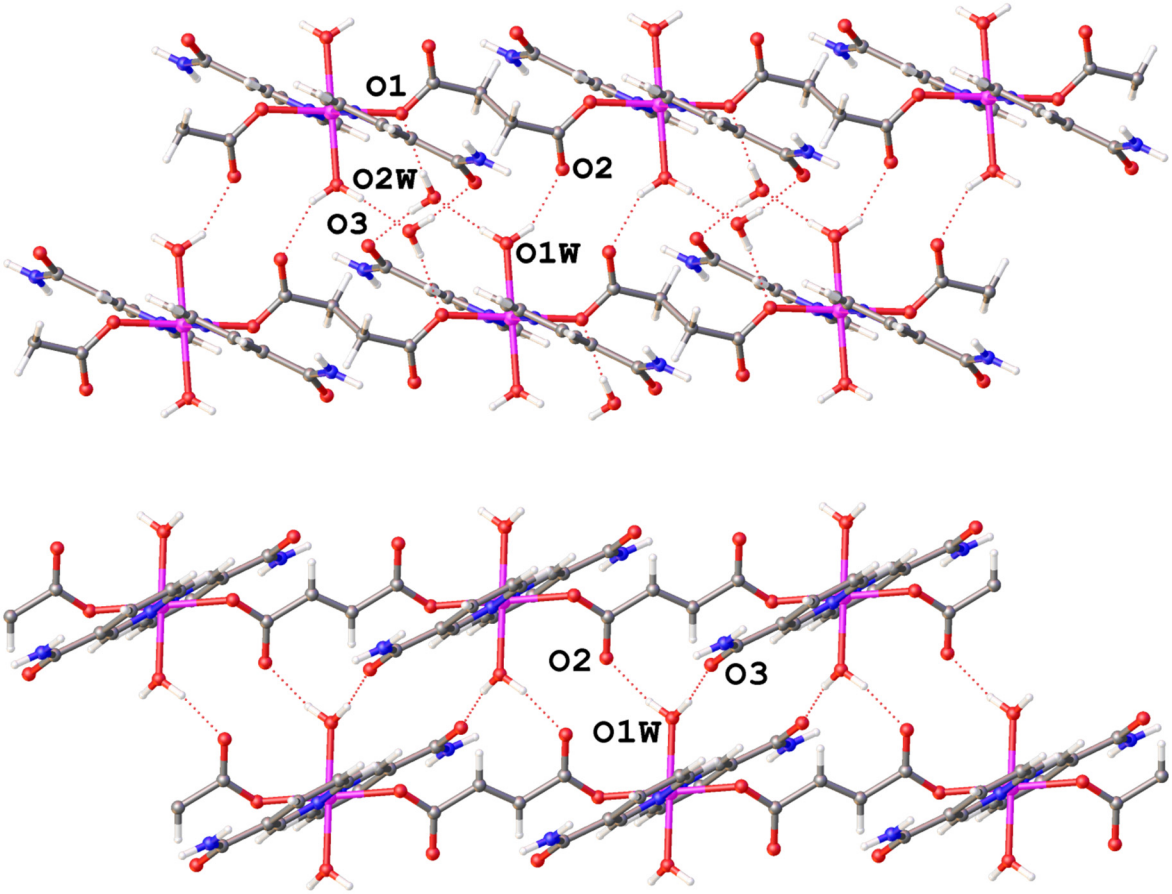

Figure S1 Comparison of O–H···O hydrogen bonds in crystal structure of the complexes **I** (top) and **II** (bottom).

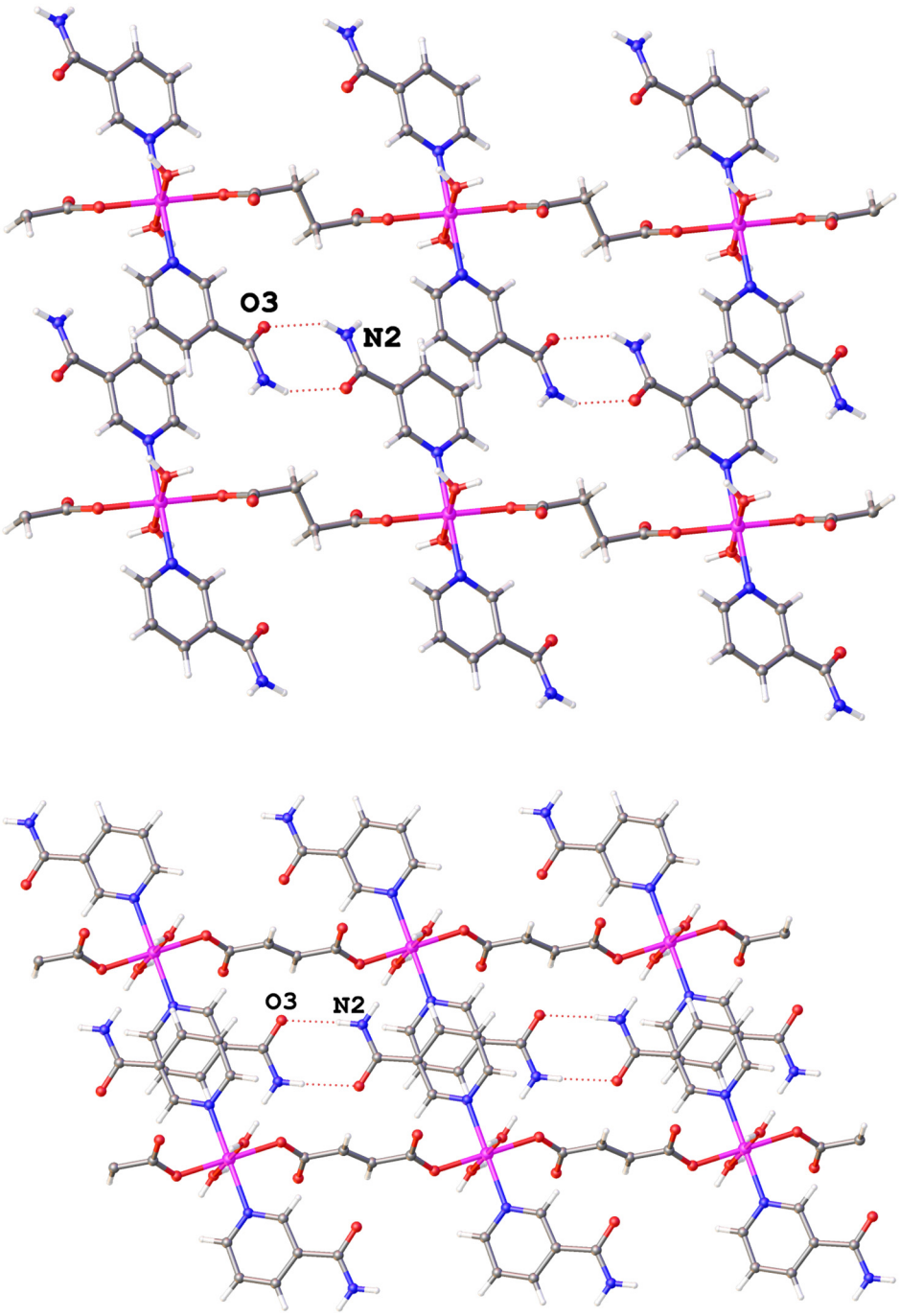

Figure S2 Comparison of face-to-face supramolecular synthons through N–H···O hydrogen bonds of carboxamide groups of two nicotinamide ligands in crystal structure of the complexes **I** (top) and **II** (bottom).

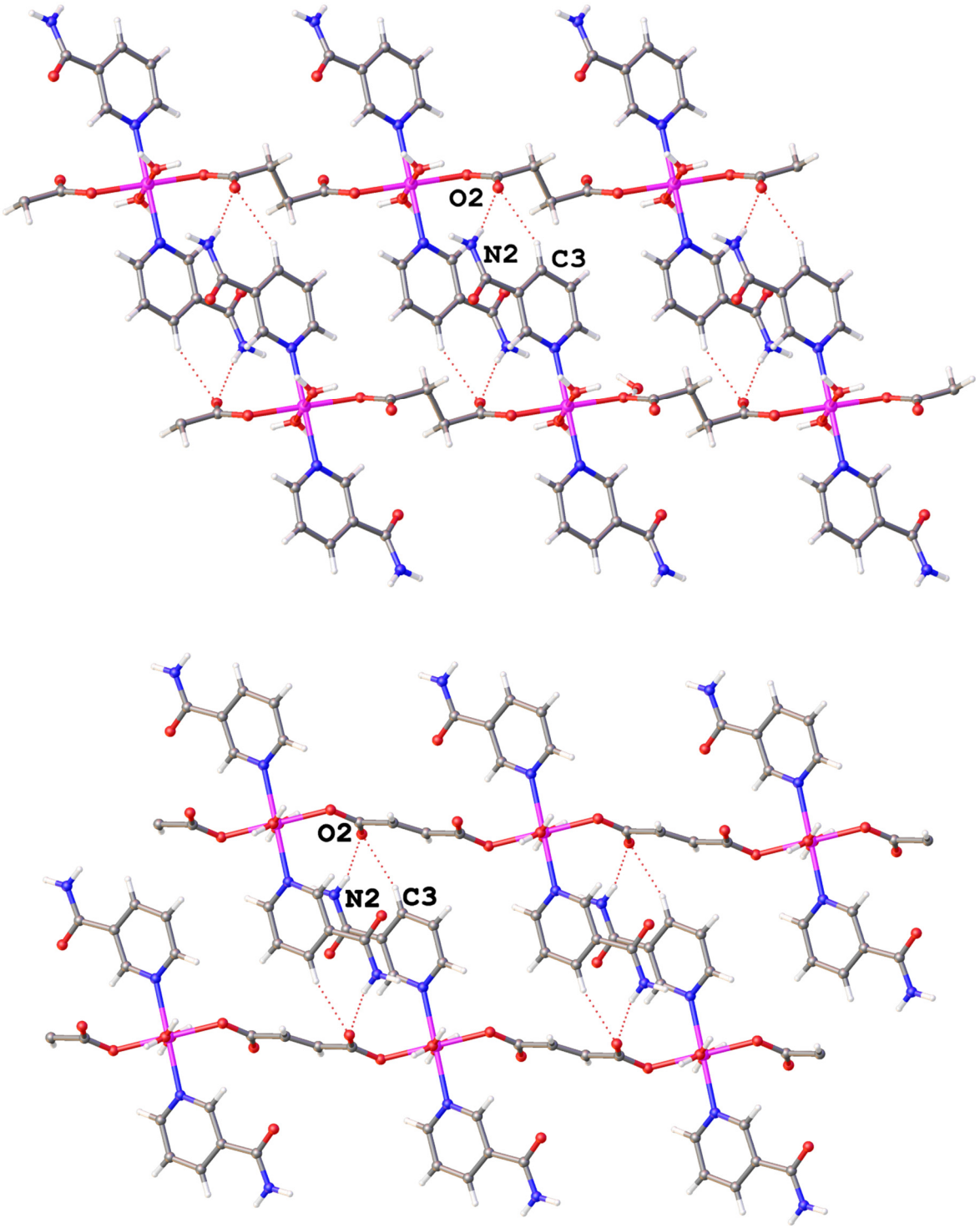

Figure S3 Comparison of N–H···O and C–H···O hydrogen bonds in crystal structure of the complex **I** (top) and the **II** (bottom)

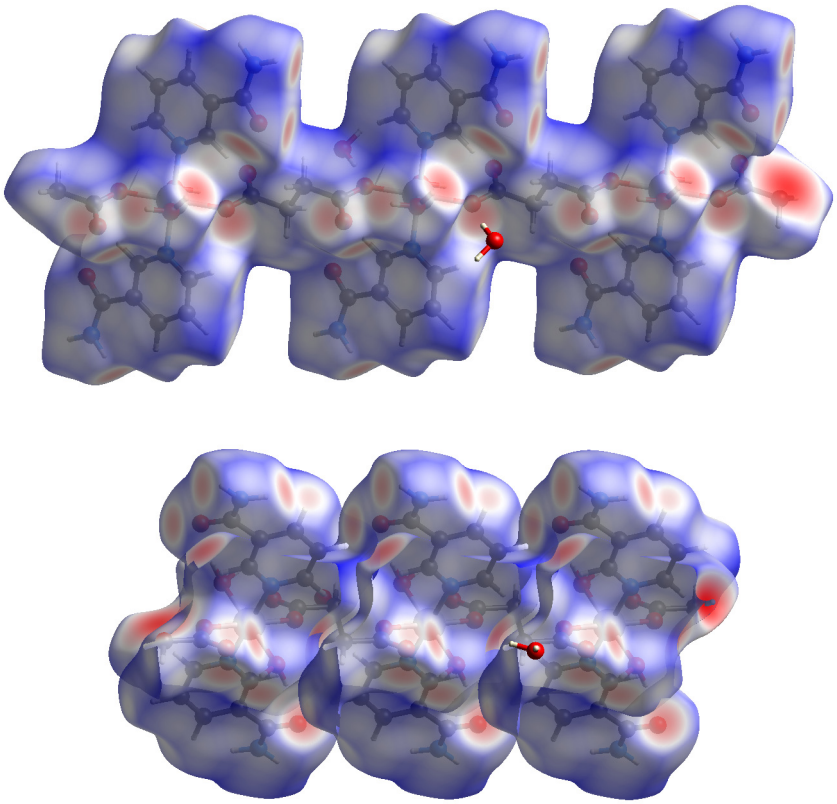

Figure S4 View of the three-dimensional Hirshfeld surface of **I** plotted over d_{norm} in the range -1.2390 + 1.1257 a.u.

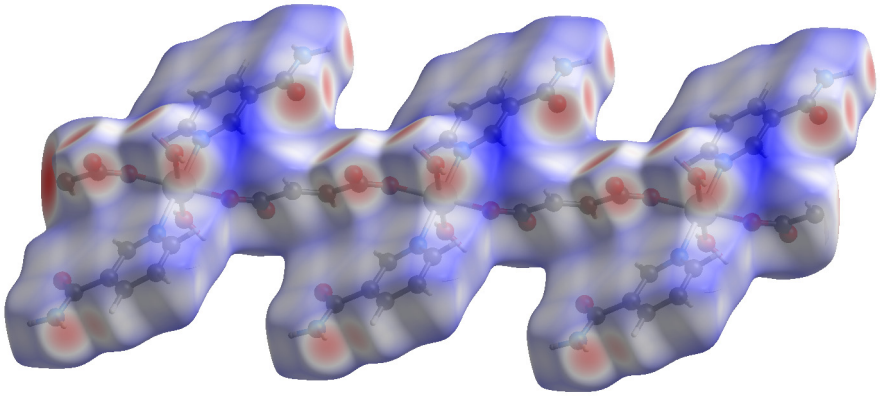

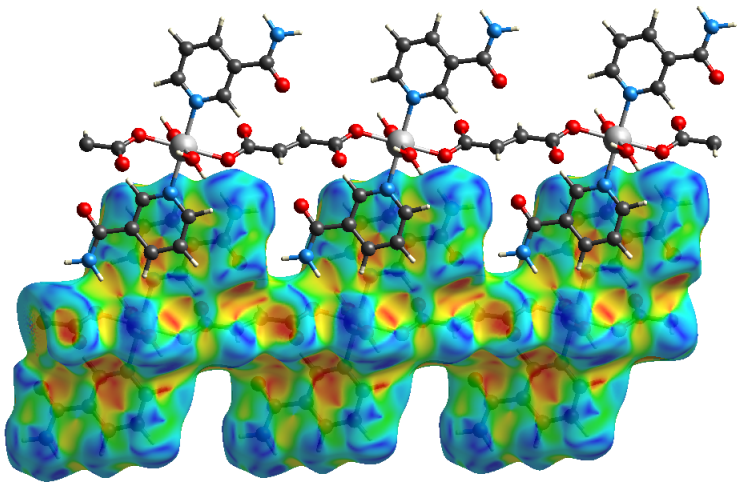

Figure S5 View of the three-dimensional Hirshfeld surface of **II** plotted over d_{norm} in the range -1.2217 + 1.4341 a.u.

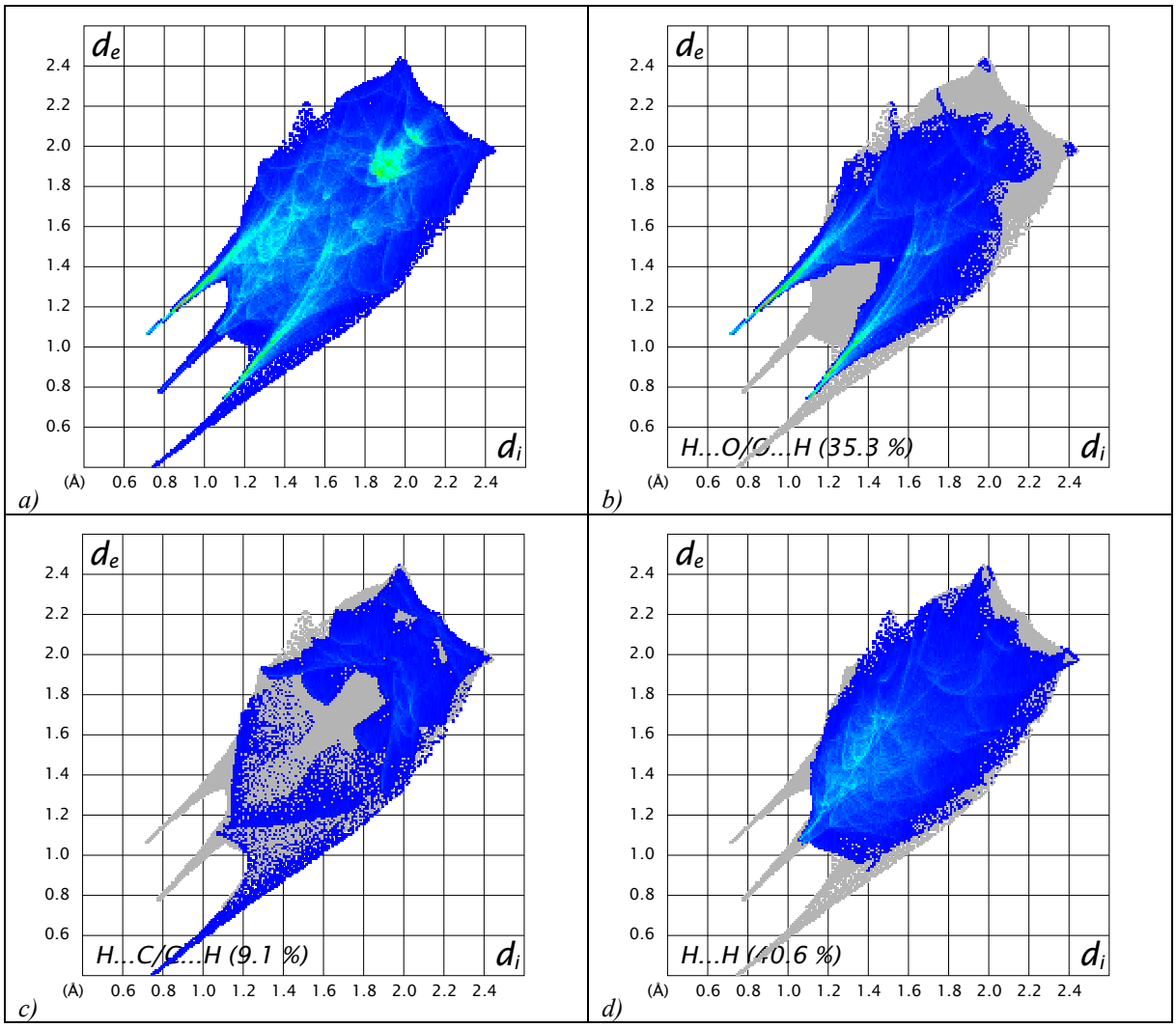

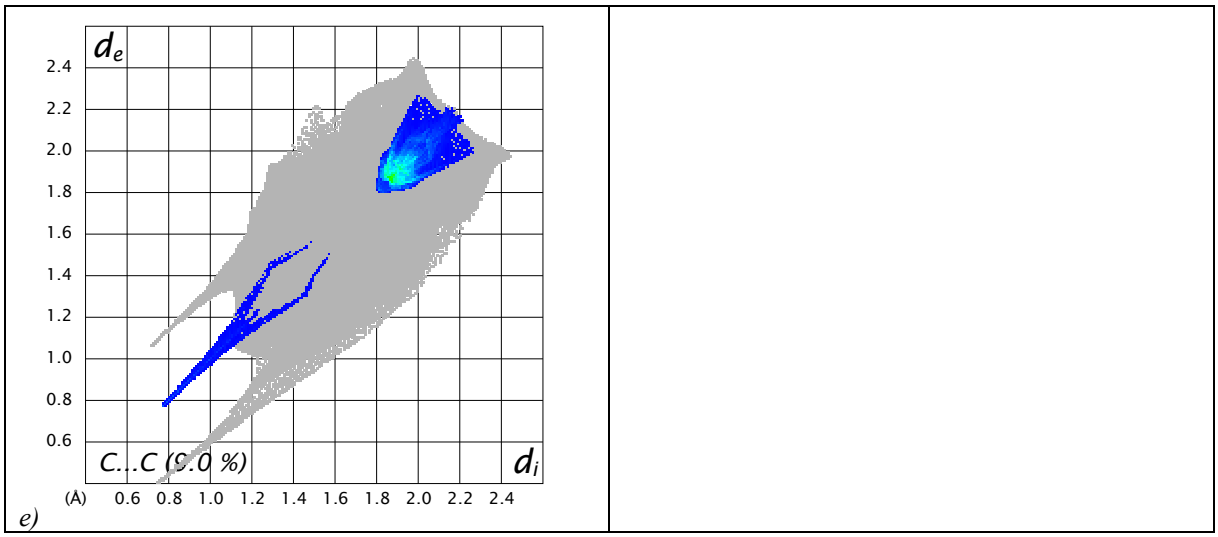

Figure S6 The full two-dimensional fingerprint plots of **I**, showing (*a*) all interactions, and delineated into (*b*) H···O/O···H, (*c*) H···Cl/Cl···H, (*d*) H···C/C···H, (*e*) O···O, and (*f*) H···H interactions. The d_i and d_e values are the closest internal and external distances from given on the Hirshfeld surface contacts.

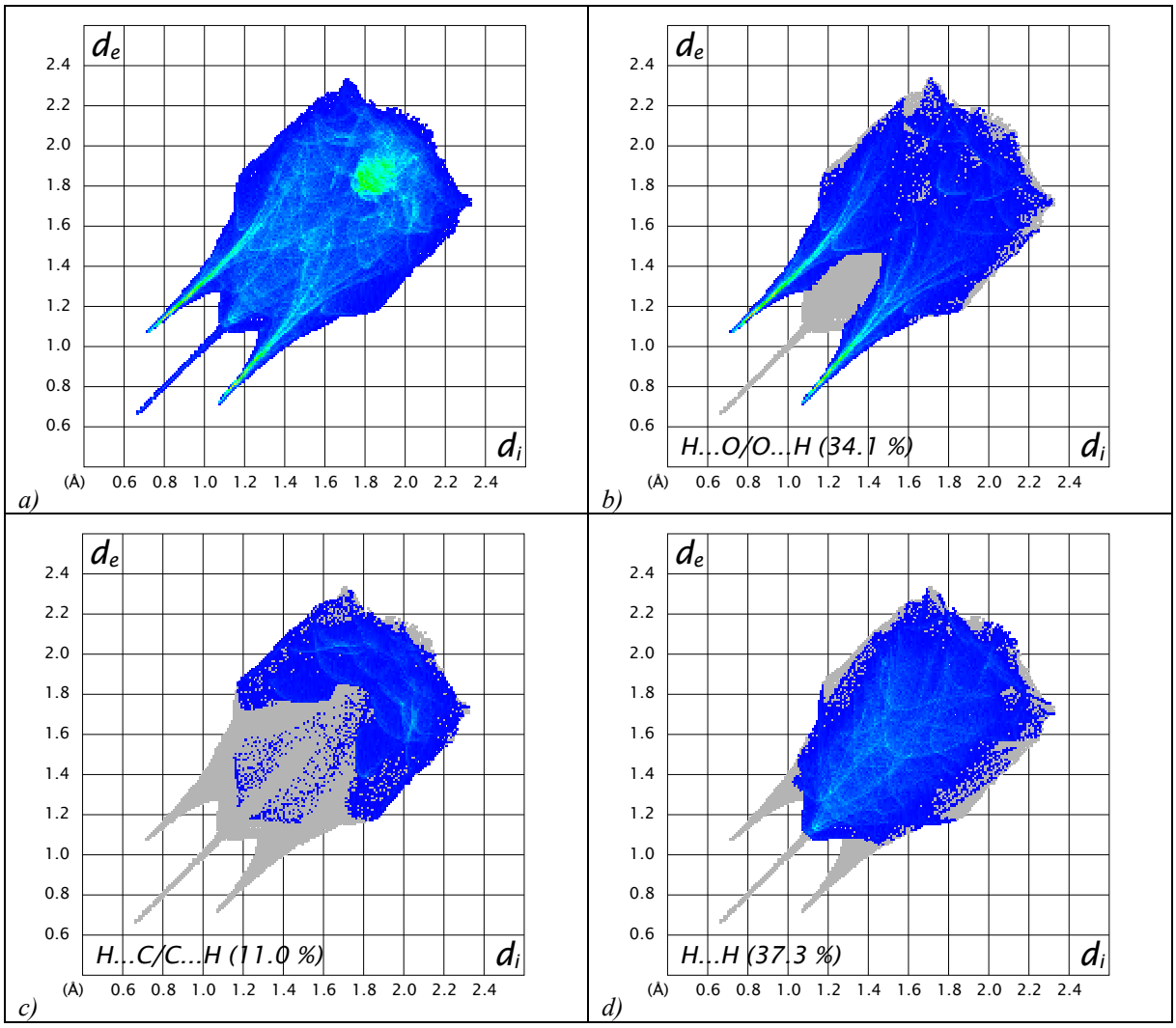

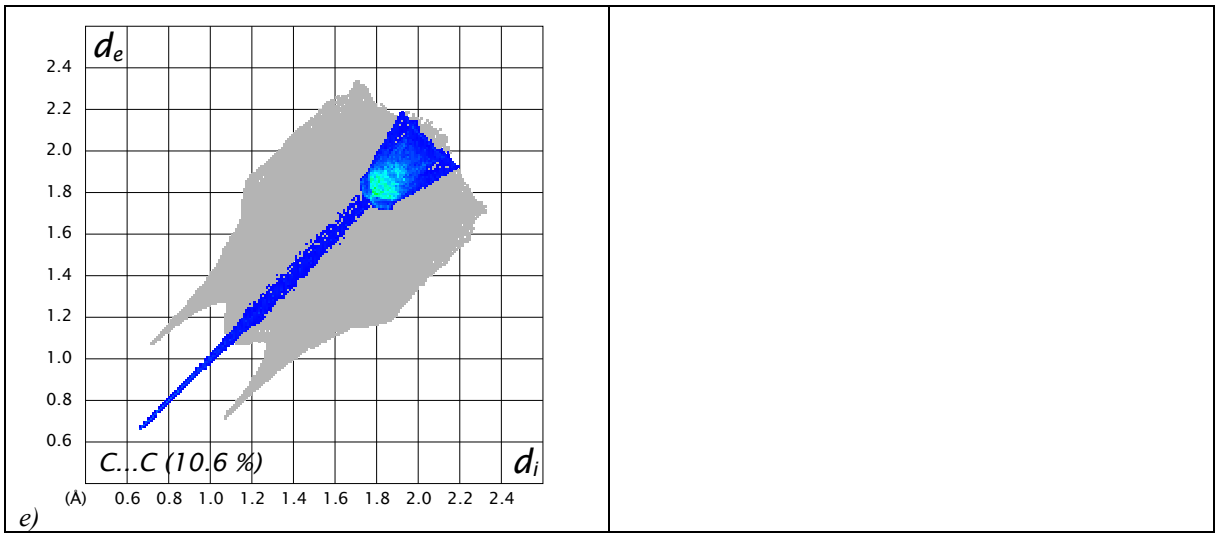

Figure S7 The full two-dimensional fingerprint plots of **II**, showing (*a*) all interactions, and delineated into (*b*) H···O/O···H, (*c*) H···Cl/Cl···H, (*d*) H···C/C···H, (*e*) O···O, and (*f*) H···H interactions. The d_i and d_e values are the closest internal and external distances from given on the Hirshfeld surface contacts.

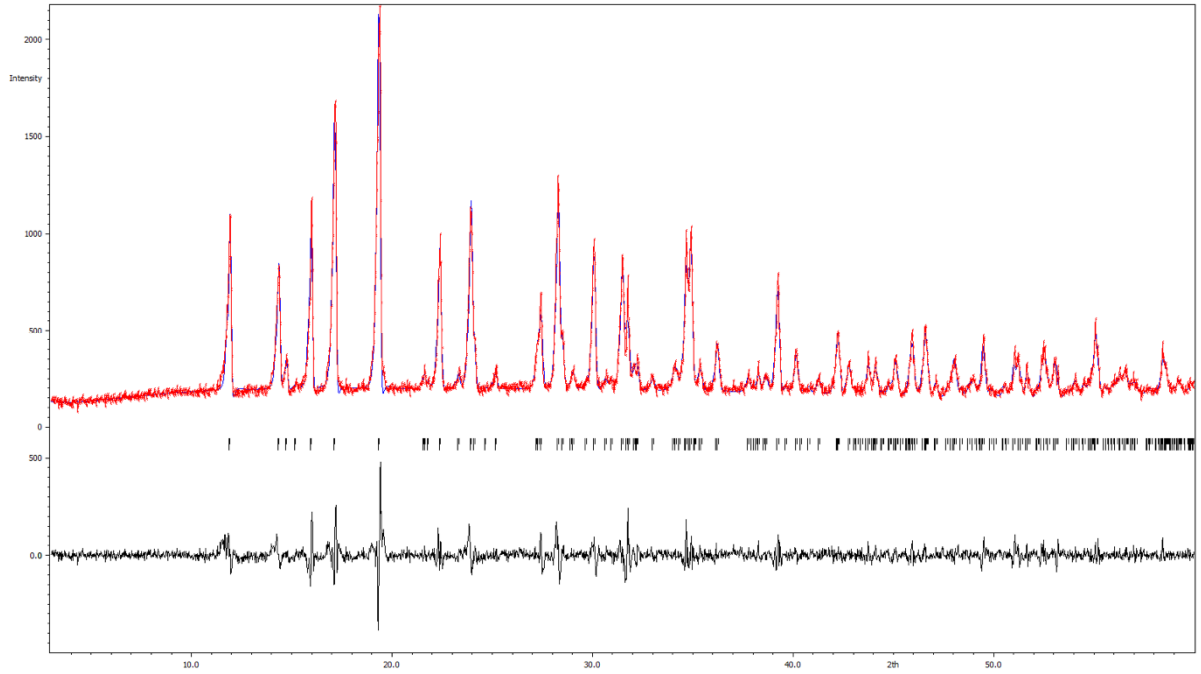

Figure S8 Observed (crosses), calculated (solid line) diffraction patterns and difference plot (below) for Le Bail analysis of **I**.

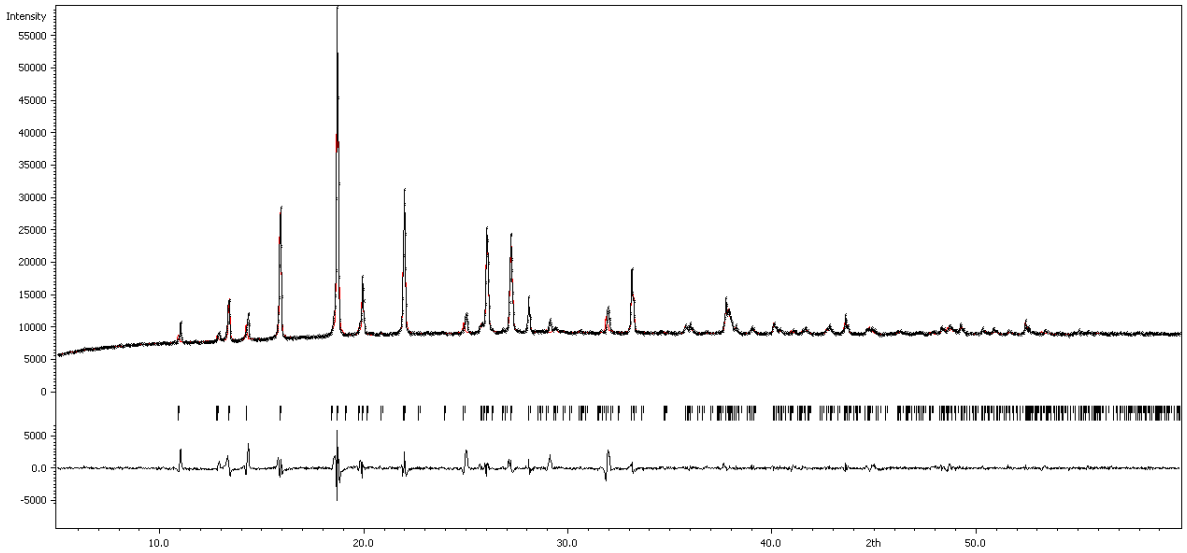

Figure S9 Observed (crosses), calculated (solid line) diffraction patterns and difference plot (below) for Le Bail analysis of **II.**

S2 Spectroscopic Characterization

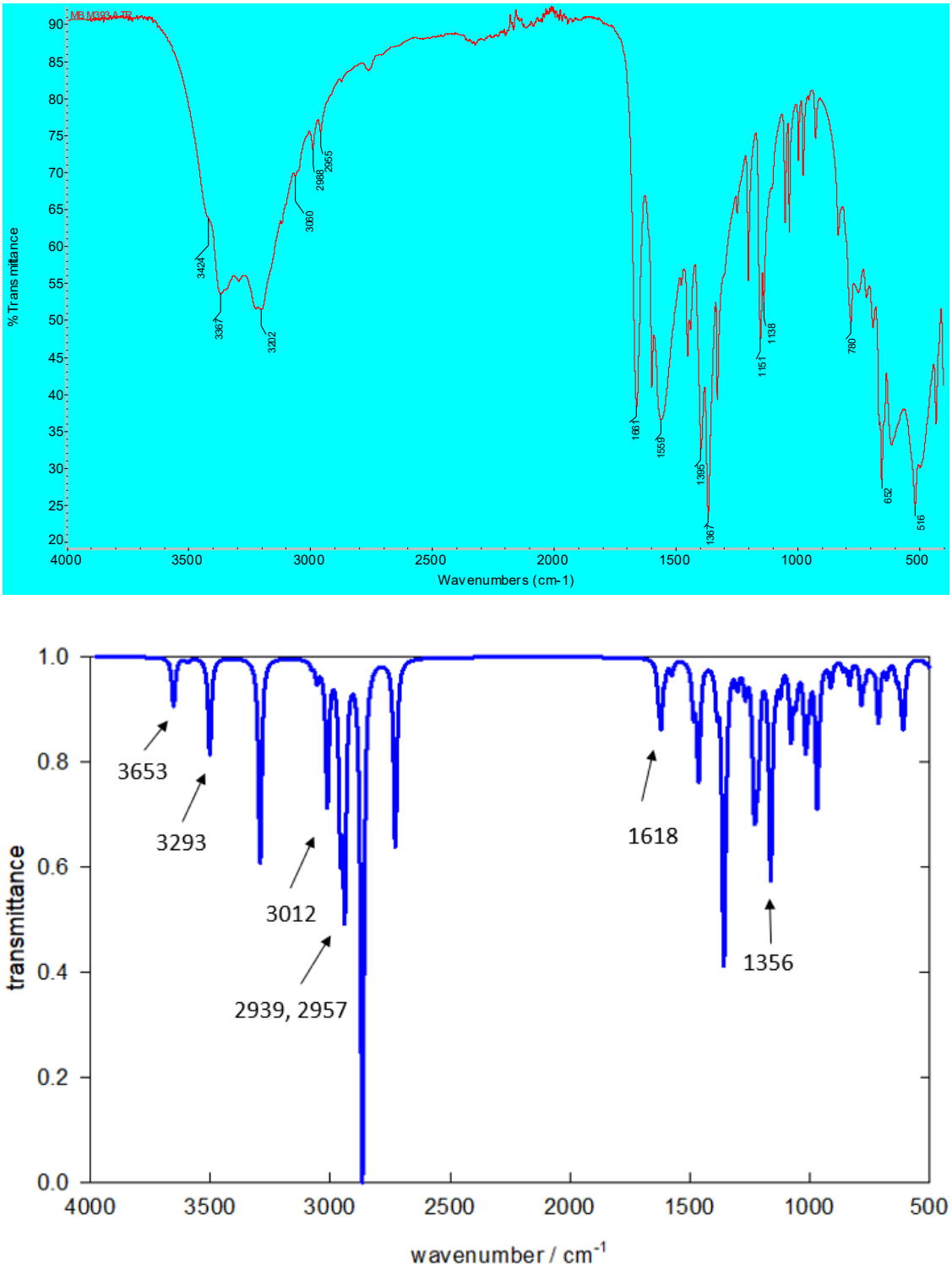

Figure S10 IR spectra of complex **I** prepared from nia, top: experiment, bottom: calculation.

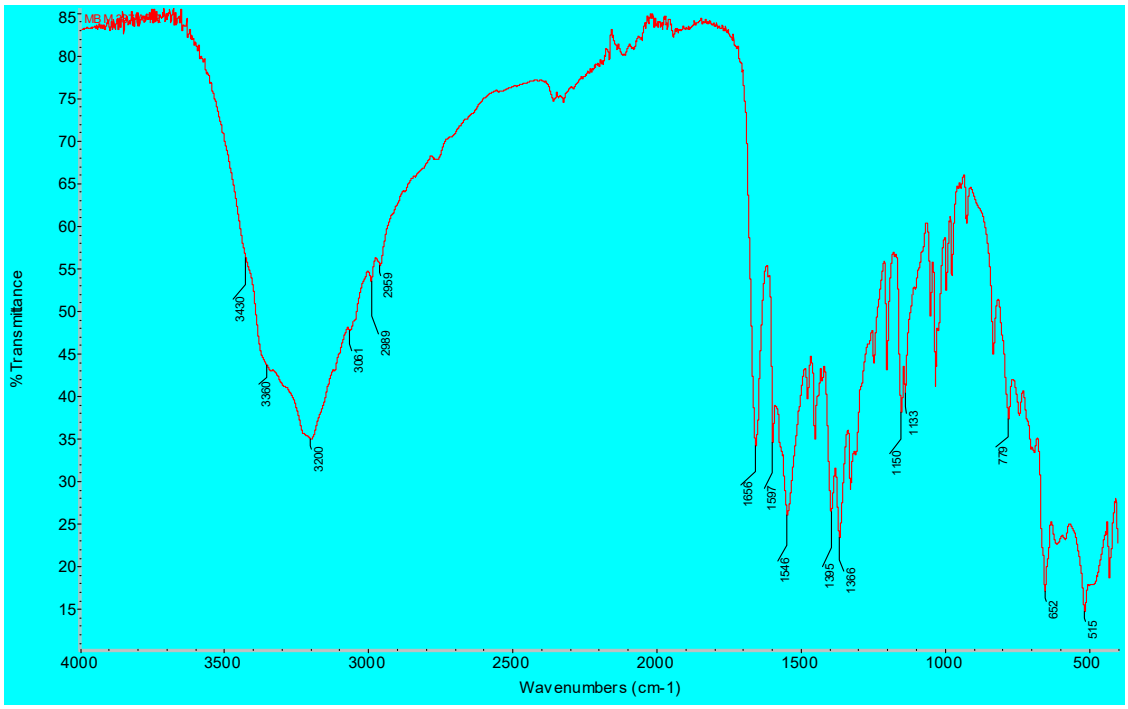

Figure S11 IR spectra of complex **I** prepared from hmnia.

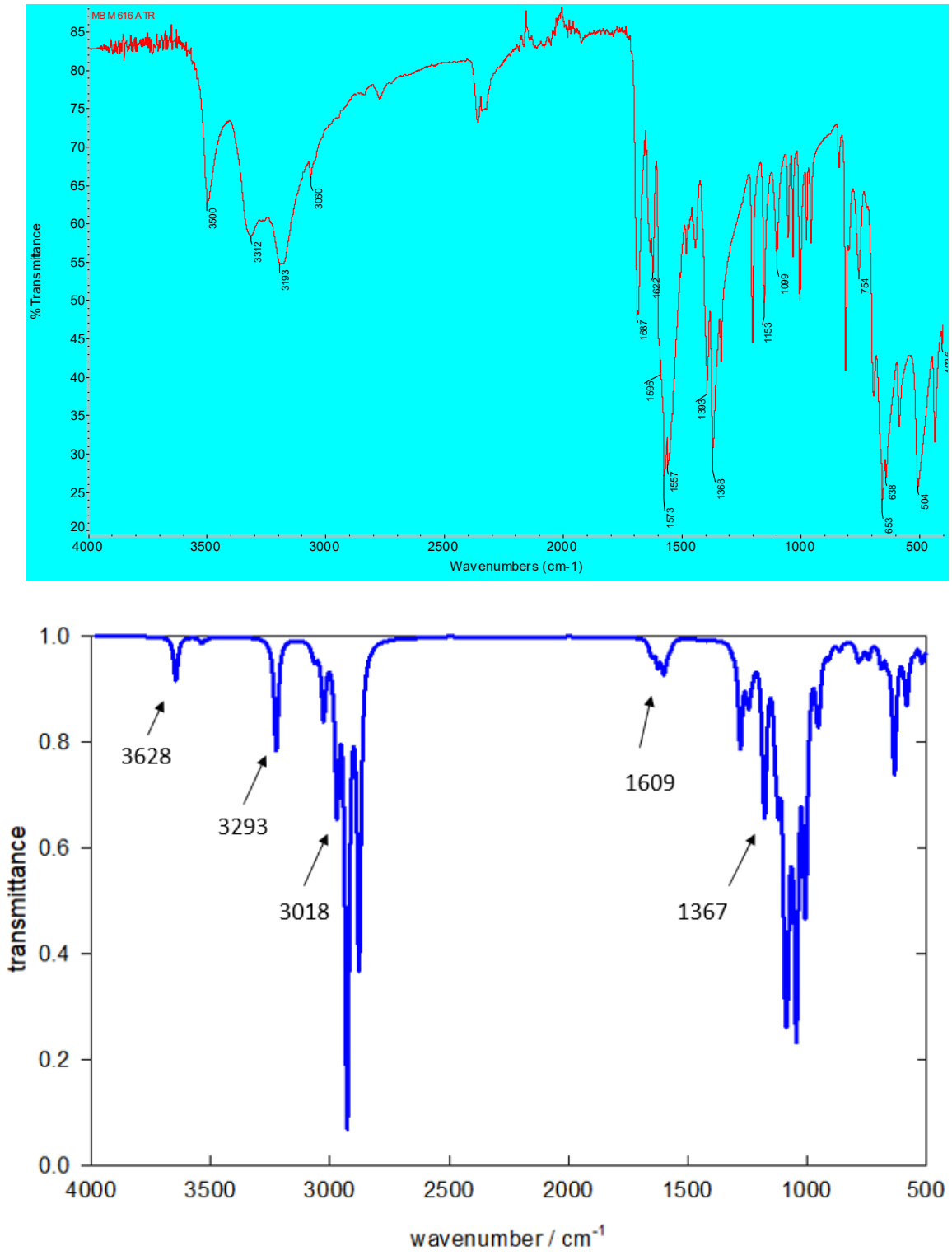

Figure S12 IR spectra of complex **II**, top: experiment, bottom: calculation.

Table S5: Characteristics bands in infrared spectra of complexes.

Compound	Water and amide group (cm^{-1})						Carboxyl group (cm^{-1})		
	ν(OH)	**$\nu_{as}(NH_2)$**	**$\nu s(NH_2)$**	**Amid I**	**Amid II**	**Amid III**	**$\nu_{as}(COO^-)$**	**$\nu_s(COO^-)$**	**Δ^b**
nia	–	3351s,br	3140s, br	1673vs 1698sh	1618s	1392 vs	–	–	–
$Na_2suc{\cdot}6H_2O$	3250-3550s, br	–	–	–	–	–	1539vs, br	1398vs, br	141
Na_2fum	–	–	–	–	–	–	1569vs, br	1381vs, br	188
complex **I** prepared from nia	3424sh	3367s,br	3202s, br	1661vs	1625sh	1395 vs	1559vs, br	1367vs, br	192
complex **I** prepared from hmnia	3430sh	3360s,br	3200vs,br	1656vs	1627sh	1395 vs	1546vs, br	1366vs, br	180
complex **II**	3500s	3312s,br	3193s, br	1687s	1622	1393 s	1573vs 1557vs	1368vs	201

[a] vs, very strong; s, strong; sh, shoulder; br, broad; [b] $\Delta = \nu_{as}(COO^-) - \nu_s(COO^-)$

Table S6: Comparison of the observed and calculated vibrational mode frequencies for the complexes I and II.

Assignment	Experimental IR (cm^{-1})		B3LYP/def2-TZVP (cm^{-1})	
	Complex **I**	Complex **II**	Complex **I**	Complex **II**
$\nu_{as}(OH)$	3424	3500	3653	3628
$\nu_{as}(NH_2)$	3367	3312	-	-
$\nu_s(NH_2)$	3202	3193	3293	3293
$\nu_{ar}(C–H)$	3060	3060	3012	3018
$\nu_{as}(CH_2)$	2988	-	2957	-
$\nu_s(CH_2)$	2955	-	2939	-
Amid I	1661	1687	-	-
Amid II	1625	1622	1618	1609
Amid III	1395	1393	1356	1367
$\nu_{as}(COO^-)$	1559	1557	-	-
$\nu_s(COO^-)$	1367	1368	-	-

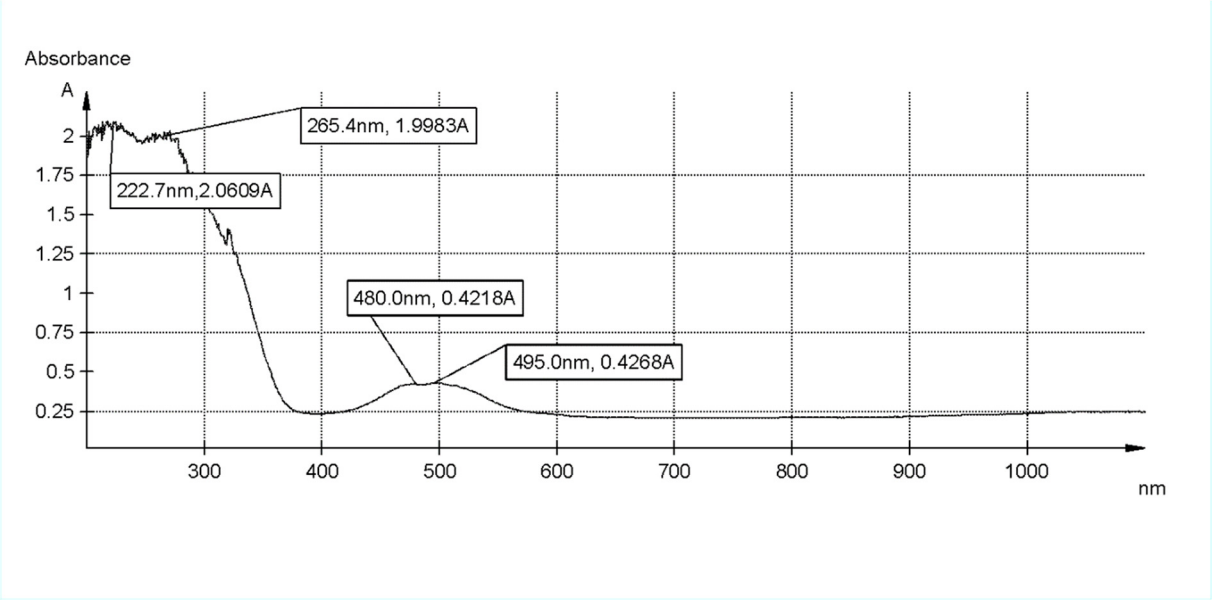

Figure S13 The electronic spectra of complex **I** prepared from nia.

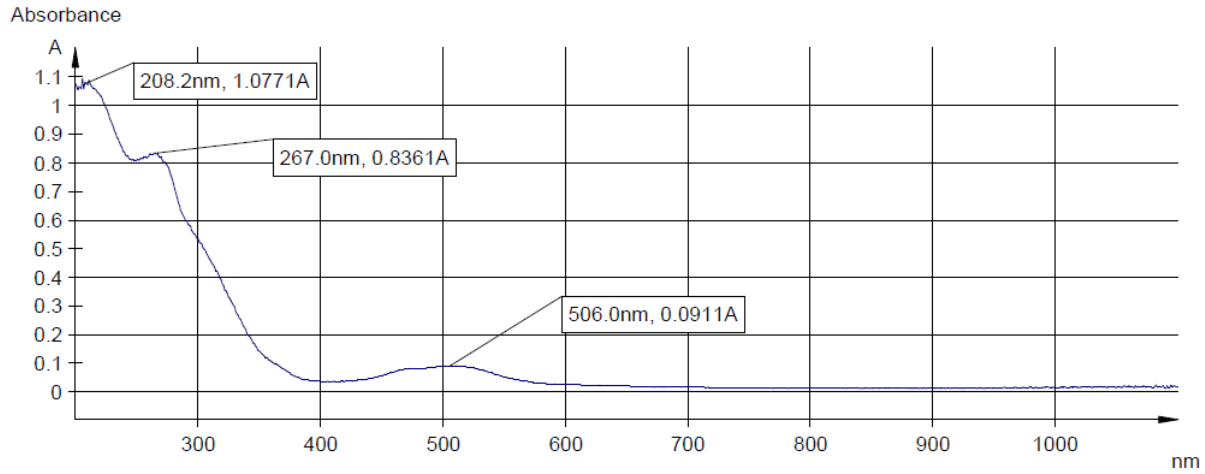

Figure S14 The electronic spectra of complex **I** prepared from hmnia.

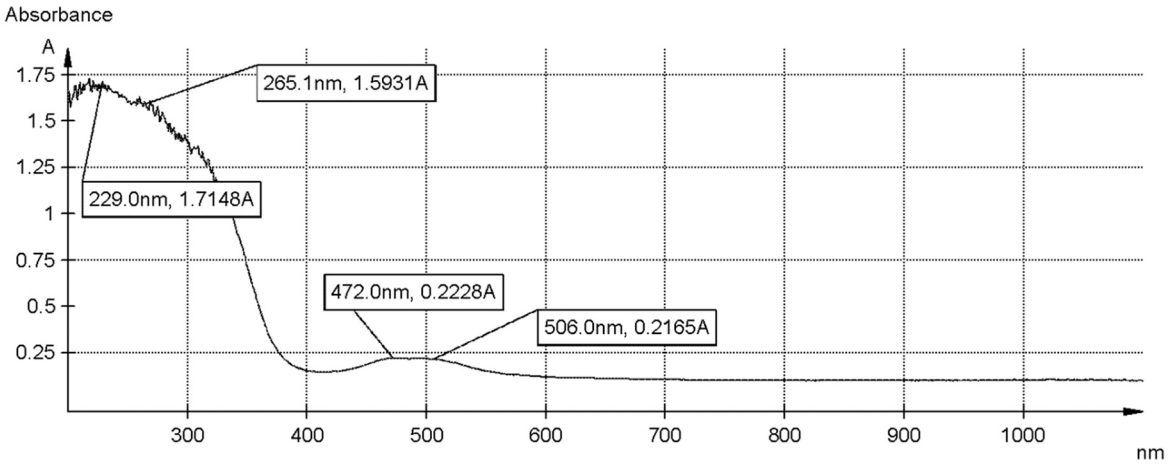

Figure S15 The electronic spectra of complex **II**.

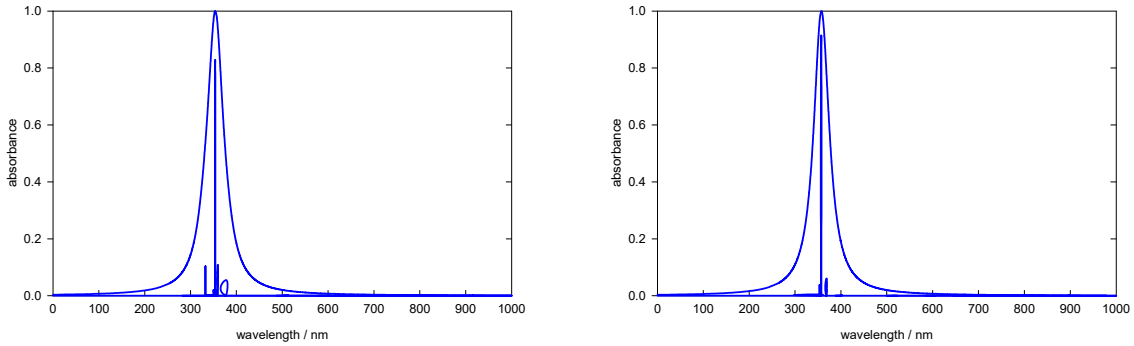

Figure S16 Calculated electron spectrum of model molecule **1** (left) and **2** (right).

Table S7 Wavelengths and relative intensities of selected calculated transitions in **1** and **2**.

	transition number	λ/nm$_o$	f_{osc}
complex **1**	**14**	332.6	0.001
	11	353.8	0.016
	9	359.4	0.002
	7	377.7	0.002
complex **2**	**9**	368.8	0.002
	11	357.3	0.021

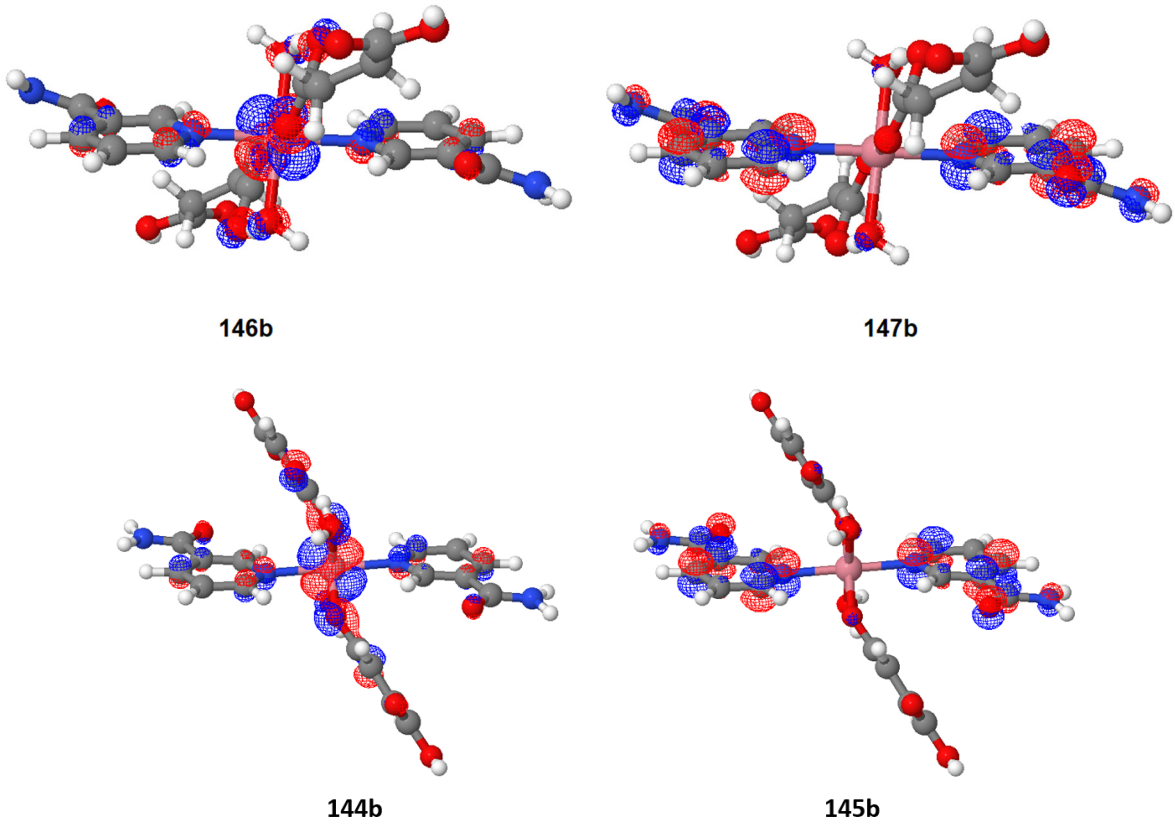

Figure S17 NTOs corresponding to the most intense transition in electron spectra of **1** (top) and **2** (bottom).

S3 Computational Characterization

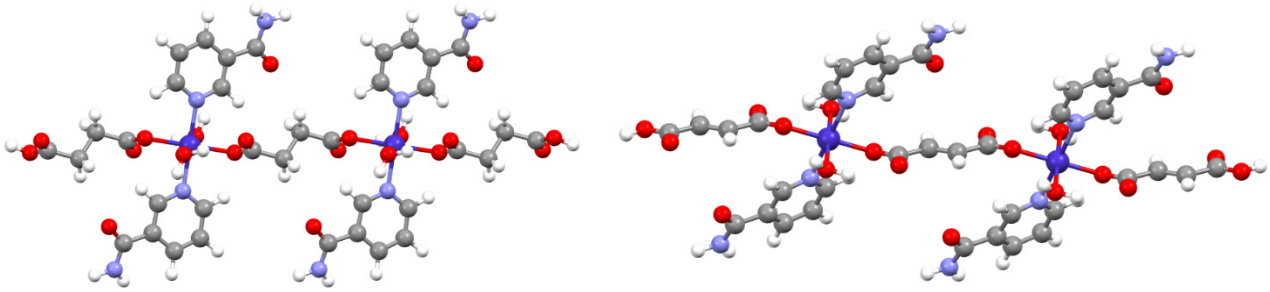

Figure S18 Model molecules **11** (left) and **22** (right).

Table S8 Parameters of magnetic coupling interaction in cm^{-1} for model systems **11** and **22** assessed by various DFT methods.

	11	**22**
B3LYP	-0.034	-0.033
PBE0	-0.023	-0.021
TPSSh	-0.062	-0.075

Table S9. Calculated relative energy levels of all Kramers' doublets of ground term $^4T_{1g}$ in model molecules **1** and **2**.

Model molecule	$E(\Gamma_a)/cm^{-1}$	$E(\Gamma_b)/cm^{-1}$	$E(\Gamma_c)/cm^{-1}$	$E(\Gamma_d)/cm^{-1}$	$E(\Gamma_e)/cm^{-1}$	$E(\Gamma_f)/cm^{-1}$
1	0.0	215.2	635.3	940.8	1580.9	1666.7
2	0.0	250.2	523.1	885.8	1322.7	1420.4

S4 Dynamic Magnetic Properties

The magnetic data induced by the oscillating; alternating-current (AC) magnetic field were obtained at an amplitude of B_{AC} = 0.30 mT. Collected sets of χ' and χ'' (susceptibilities (16 χ' and 16 χ'') at each temperature were fitted using the formulas for extended one-set Debye model

$$\chi'(\omega) = \chi_S + (\chi_T - \chi_S)\frac{1+(\omega\tau)^{(1-\alpha)}\sin(\pi\alpha/2)}{1+2(\omega\tau)^{(1-\alpha)}\sin(\pi\alpha/2)+(\omega\tau)^{(2-2\alpha)}} \quad \textbf{(S1)}$$

$$\chi''(\omega) = (\chi_T - \chi_S)\frac{(\omega\tau)^{(1-\alpha)}\cos(\pi\alpha/2)}{1+2(\omega\tau)^{(1-\alpha)}\sin(\pi\alpha/2)+(\omega\tau)^{(2-2\alpha)}} \quad \textbf{(S2)}$$

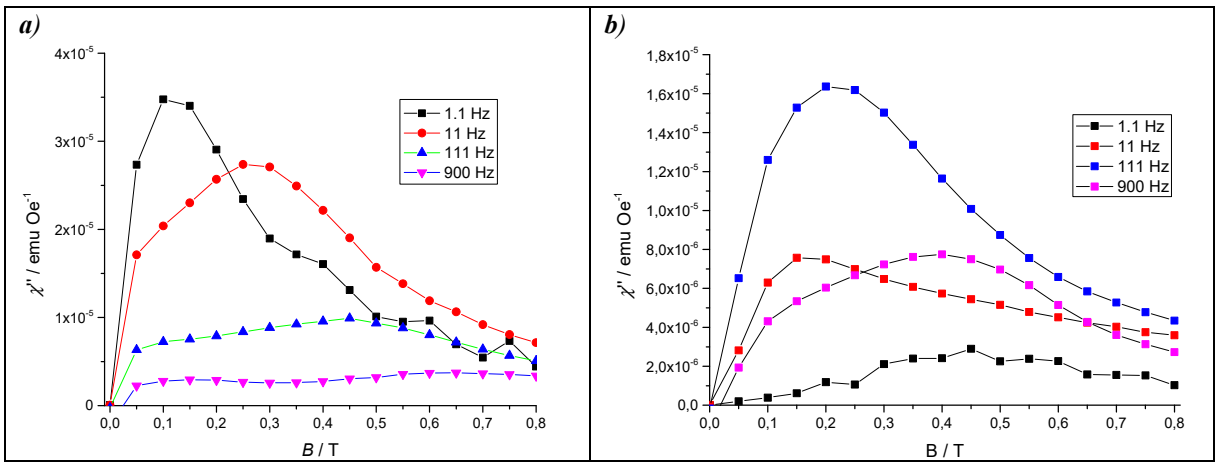

Figure S19 Mapping of the out-of-phase susceptibility components χ'' of **I** (***a***) and **II** (***b***) as a function of the applied external B_{DC} field for a set of four frequencies of B_{AC} field at T=2.0 K.

Table S10 Conditions of AC magnetic experiments for compound **I**.

B_{DC} / T	B_{AC} / mT	Temperature range	Frequency range
0.02	3.0	1.8-6.4 K (26 steps)	1.0 Hz -959.8 Hz (16 steps)
0.10	3.0	1.8-8.0 K (32 steps)	1.0 Hz -959.8 Hz (16 steps)

Table S11 Conditions of AC magnetic experiments for compound **II**.

B_{DC} / T	B_{AC} / mT	Temperature range	Frequency range
0.05	3.0	1.8-6.0 K (22 steps)	1.0 Hz -959.8 Hz (16 steps)
0.10	3.0	1.8-6.0 K (22 steps)	1.0 Hz -959.8 Hz (16 steps)
0.15	3.0	1.8-6.0 K (22 steps)	1.0 Hz -959.8 Hz (16 steps)
0.20	3.0	1.8-6.0 K (22 steps)	1.0 Hz -959.8 Hz (16 steps)

Table S12 Parameters of the extended one-set Debye model (eq. S1 and S2) for **I** measured at 0.02 T.

T /K	χ_T /10^{-6} m^3 mol^{-1}	χ_S /10^{-6} m^3 mol^{-1}	α	τ /10^{-3} s	R^2
1.8	4.6(1)	3.14(1)	0.32(3)	73(12)	0.99965
2.0	4.13(7)	2.83(1)	0.30(3)	55(7)	0.99966
2.2	3.73(5)	2.570(8)	0.27(3)	43(5)	0.99968
2.4	3.41(4)	2.366(8)	0.25(3)	35(3)	0.99968
2.6	3.14(3)	2.191(7)	0.23(3)	28(2)	0.99969
2.8	2.91(3)	2.041(7)	0.21(3)	23(2)	0.99969
3.0	2.72(2)	1.910(6)	0.19(3)	19(1)	0.99969
3.2	2.55(2)	1.796(6)	0.17(2)	14.8(8)	0.99970
3.4	2.40(2)	1.695(5)	0.15(2)	11.7(6)	0.99969
3.6	2.27(1)	1.605(5)	0.12(2)	9.2(4)	0.99970
3.8	2.15(1)	1.524(5)	0.10(2)	7.0(3)	0.99971
4.0	2.040(9)	1.452(5)	0.08(2)	5.4(2)	0.99973
4.2	1.943(8)	1.386(5)	0.06(2)	4.0(1)	0.99973
4.4	1.855(7)	1.328(4)	0.04(2)	3.0(1)	0.99974
4.6	1.776(6)	1.274(4)	0.03(2)	2.25(7)	0.99976
4.8	1.702(5)	1.225(4)	0.01(2)	1.68(5)	0.99977
5.0	1.636(5)	1.181(4)	0.002(17)	1.25(3)	0.99978
5.2	1.575(4)	1.139(3)	0.00(0)	0.94(2)	0.99979
5.4	1.519(4)	1.102(4)	0.000(4)	0.71(2)	0.99979
5.6	1.467(4)	1.066(4)	0.00(0)	0.53(1)	0.99979
5.8	1.420(4)	1.030(8)	0.01(2)	0.40(1)	0.99978
6.0	1.375(4)	0.99(1)	0.03(2)	0.30(1)	0.99979
6.2	1.333(3)	0.94(2)	0.06(3)	0.21(1)	0.99980
6.4	1.293(3)	0.86(3)	0.06(3)	0.13(1)	0.99984
6.6	1.255(3)	0.73(6)	0.13(3)	0.07(1)	0.99989
6.8	1.219(2)	0.3(3)	0.16(3)	0.02(1)	0.99992

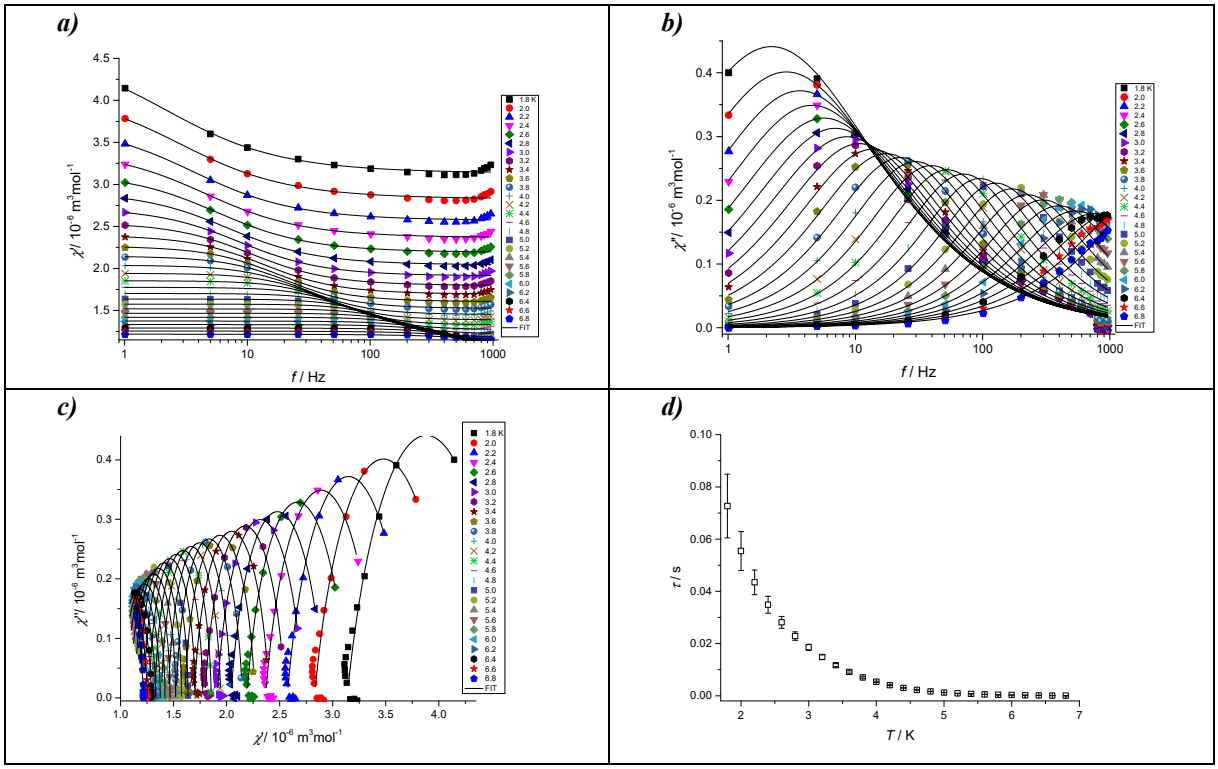

Figure S20 AC susceptibility data for **I** recorded at various temperatures at 0.02 T: Frequency dependent in-phase χ'(*a*) and out-of-phase χ''(*b*) component of AC susceptibility and Cole-Cole diagram (*c*) (solid lines are results of fits according to equations S1 and S2). Temperature dependency of relaxation time τ with standard errors

Table S13 Parameters of the extended one-set Debye model (eq. S1 and S2) for **I** measured at 0.1 T.

T /K	χ_T / 10^{-6} m^3 mol^{-1}	χ_S / 10^{-6} m^3 mol^{-1}	α	τ / 10^{-3} s	R^2
1.8	5.2(2)	0.41(1)	0.39(1)	165(17)	0.99752
2.0	4.7(1)	0.381(9)	0.38(1)	135(12)	0.99801
2.2	4.1(1)	0.36(1)	0.36(1)	100(8)	0.99760
2.4	3.6(1)	0.35(1)	0.32(2)	72(5)	0.99645
2.6	3.22(7)	0.334(9)	0.30(1)	54(3)	0.99710
2.8	2.98(6)	0.320(9)	0.27(1)	43(2)	0.99688
3.0	2.70(4)	0.304(8)	0.26(1)	33(1)	0.99774
3.2	2.52(4)	0.296(9)	0.22(1)	26(1)	0.99693
3.4	2.34(3)	0.283(7)	0.20(1)	19.7(6)	0.99798
3.6	2.22(2)	0.273(7)	0.18(1)	15.3(4)	0.99807
3.8	2.06(2)	0.263(7)	0.15(1)	11.0(3)	0.99840
4.0	1.96(1)	0.255(6)	0.121(9)	8.1(2)	0.99883
4.2	1.875(9)	0.242(4)	0.113(7)	6.03(8)	0.99943
4.4	1.775(8)	0.235(4)	0.088(7)	4.33(5)	0.99944
4.6	1.698(6)	0.227(4)	0.076(6)	3.16(3)	0.99960
4.8	1.617(5)	0.219(4)	0.061(5)	2.28(2)	0.99967
5.0	1.552(5)	0.213(4)	0.047(5)	1.66(1)	0.99963
5.2	1.495(2)	0.204(3)	0.043(4)	1.220(9)	0.99976
5.4	1.437(2)	0.199(3)	0.034(3)	0.903(4)	0.99987
5.6	1.393(2)	0.191(3)	0.031(3)	0.677(3)	0.99988
5.8	1.343(2)	0.187(4)	0.024(4)	0.509(3)	0.99982
6.0	1.300(2)	0.179(5)	0.022(4)	0.386(2)	0.99986
6.2	1.262(2)	0.174(6)	0.019(5)	0.296(2)	0.99984
6.4	1.218(2)	0.168(9)	0.014(6)	0.227(2)	0.99983
6.6	1.187(3)	0.15(2)	0.019(8)	0.175(3)	0.99976
6.8	1.153(2)	0.12(2)	0.023(8)	0.133(3)	0.99987
7.0	1.123(3)	0.08(4)	0.037(1)	0.100(5)	0.99977
7.2	1.093(3)	0(1)	0.031(7)	0.0728(7)	0.99975
7.4	1.65(2)	0(0)	0.015(6)	0.0590(6)	0.99987
7.6	1.038(2)	0(0)	0.0(0)	0.0484(5)	0.99982
7.8	1.015(2)	0.000(2)	0.0(0)	0.0390(6)	0.99979
8.0	0.993(2)	0.000(0)	0.000(0)	0.0318(6)	0.99973

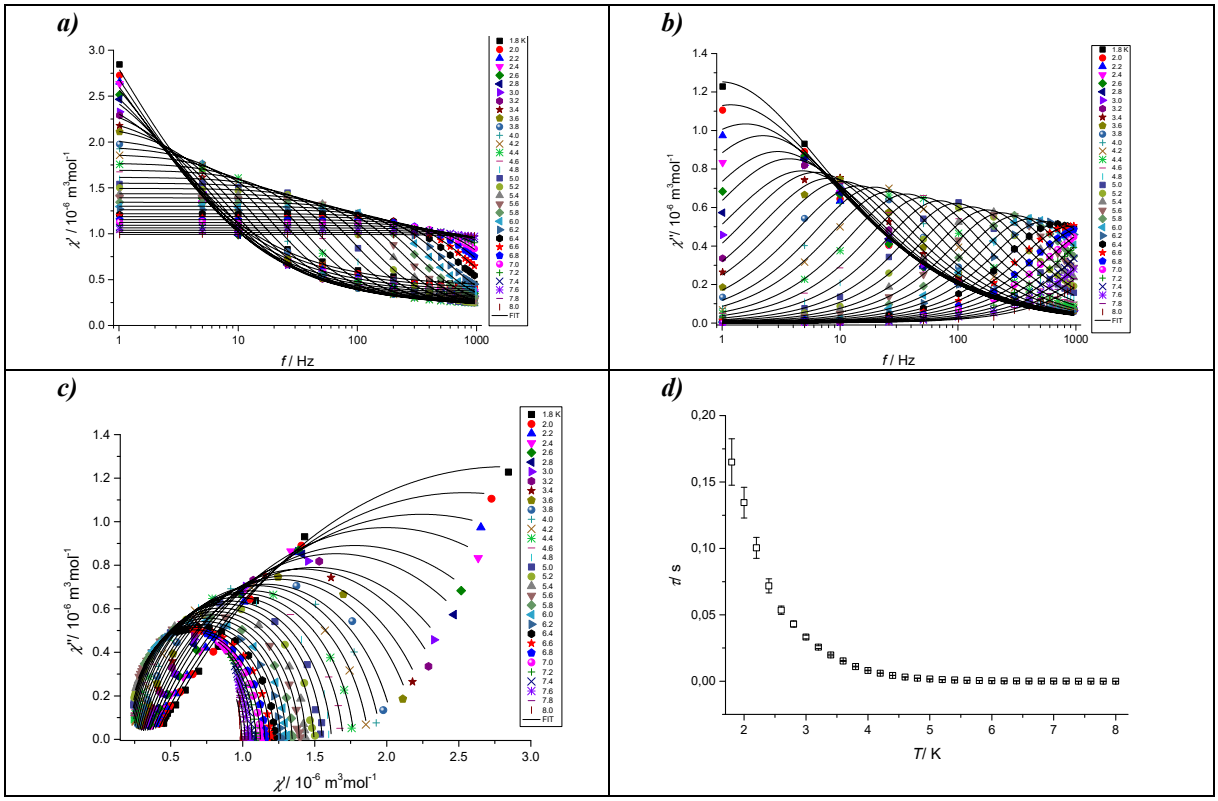

Figure S21 AC susceptibility data for **I** recorded at various temperatures at 0.1 T: Frequency dependent in-phase χ'(*a*) and out-of-phase χ''(*b*) component of AC susceptibility and Cole-Cole diagram (*c*) (solid lines are results of fits according to equations S1 and S2). Temperature dependency of relaxation time τ with standard errors

Table S14 Parameters of the extended one-set Debye model (eq. S1 and S2) for **II** measured at 0.05 T.

T/ K	χ_T/ $10^{-6}m^3$ mol^{-1}	χ_S/ $10^{-6}m^3$ mol^{-1}	α	τ/ 10^{-3} s	R^2
1.8	16.90(7)	11.30(5)	0.21(2)	2.15(8)	0.99976
2.0	15.12(6)	10.21(5)	0.20(2)	1.74(6)	0.99977
2.2	13.70(5)	9.30(5)	0.19(2)	1.43(5)	0.99977
2.4	12.56(5)	8.58(5)	0.19(2	1.20(4)	0.99977
2.6	11.60(4)	7.96(5)	0.19(2)	1.02(3)	0.99978
2.8	10.77(4)	7.41(5)	0.19(2)	0.88(3)	0.99978
3.0	10.06(3)	6.96(5)	0.19(2)	0.78(3)	0.99977
3.2	9.43(3)	6.55(5)	0.19(2)	0.67(2)	0.99977
3.4	8.89(3)	6.19(6)	0.19(2)	0.60(2)	0.99977
3.6	8.40(3)	5.86(6)	0.19(2)	0.53(2)	0.99976
3.8	7.97(3)	5.57(6)	0.19(2)	0.47(2)	0.99976
4.0	7.57(3)	5.31(7)	0.18(3)	0.42(2)	0.99975
4.2	7.22(2)	5.07(7)	0.18(3)	0.37(2)	0.99975
4.4	6.90(2)	4.85(8)	0.18(3)	0.32(2)	0.99974
4.6	6.60(2)	4.64(9)	0.17(3)	0.28(2)	0.99974
4.8	6.33(2)	4.4(1)	0.17(3)	0.24(2)	0.99974
5.0	6.08(2)	4.23(1)	0.16(4)	0.20(2)	0.99975
5.2	5.85(2)	4.01(1)	0.16(4)	0.16(2)	0.99977
5.4	5.64(2)	3.8(2)	0.16(4)	0.13(2)	0.99979
5.6	5.44(1)	3.4(2)	0.17(4)	0.09(2)	0.99983
5.8	5.26(1)	2.8(5)	0.19(4)	0.05(2)	0.99987
6.0	5.08(1)	1(2)	0.21(4)	0.02(1)	0.99990

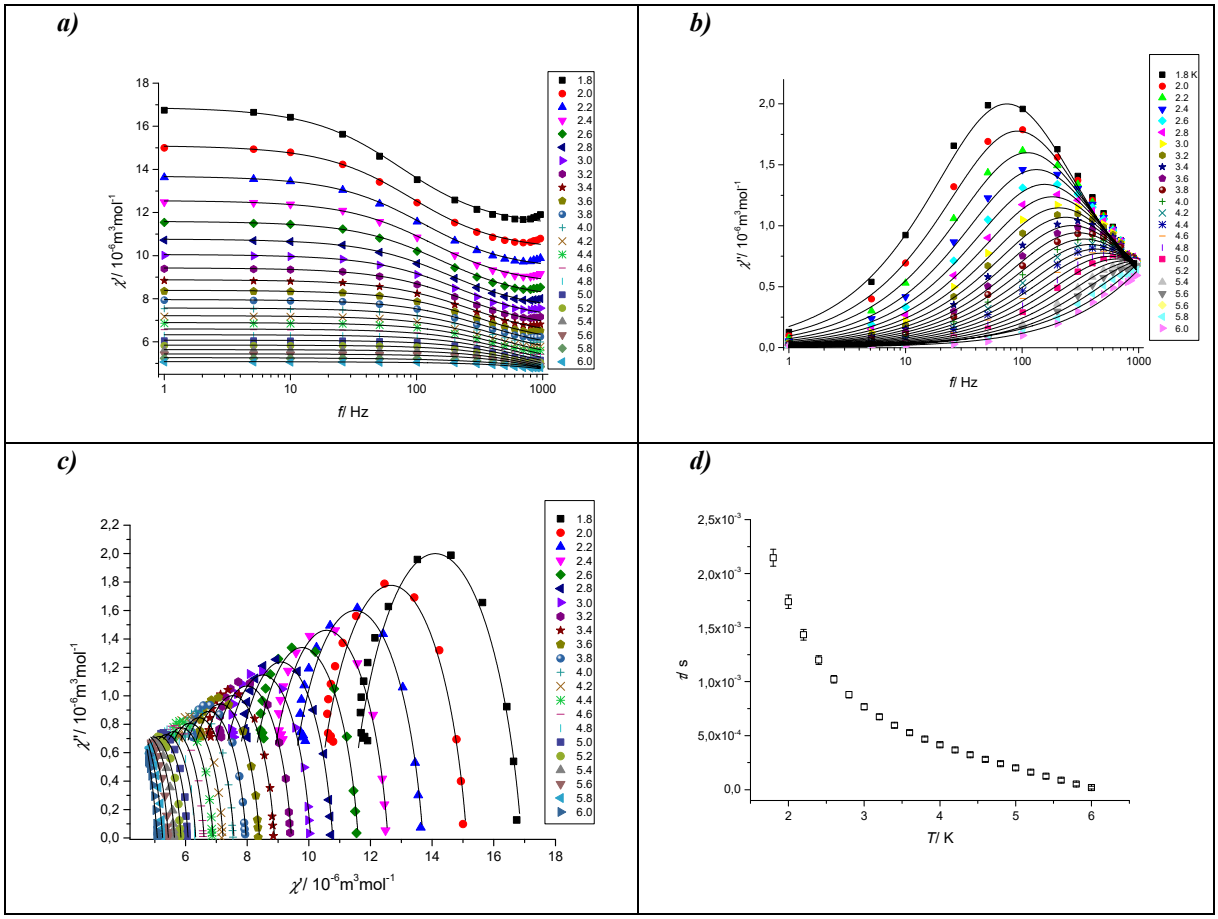

Figure S22 AC susceptibility data for **II** recorded at various temperatures at 0.05 T: Frequency dependent in-phase χ'(*a*) and out-of-phase χ''(*b*) component of AC susceptibility and Cole-Cole diagram (*c*) (solid lines are results of fits according to equations S1 and S2). Temperature dependency of relaxation time τ with standard errors

Table S15 Parameters of the extended one-set Debye model (eq. S1 and S2) for **II** measured at 0.1 T.

T/ K	χ_T/ $10^{-6}m^3mol^{-1}$	χ_S/ $10^{-6}m^3mol^{-1}$	α	τ/ $10^{-3}s$	R^2
1.8	16.70(9)	5.87(7)	0.24(1)	2.52(6)	0.99937
2.0	14.93(7)	5.36(6)	0.23(1)	2.05(5)	0.99949
2.2	13.54(6)	4.92(5)	0.227(9)	1.68(3)	0.99959
2.4	12.46(5)	4.56(5)	0.224(9)	1.41(3)	0.99965
2.6	11.51(4)	4.24(5)	0.219(9)	1.19(2)	0.99968
2.8	10.70(4)	3.98(3)	0.214(9)	1.01(2)	0.99968
3.0	10.01(7)	3.68(1)	0.23(2)	0.84(3)	0.99878
3.2	9.39(3)	3.55(4)	0.208(9)	0.77(1)	0.99973
3.4	8.85(3)	3.38(4)	0.204(9)	0.68(1)	0.99974
3.6	8.36(3)	3.21(5)	0.20(1)	0.60(1)	0.99969
3.8	7.93(2)	3.08(5)	0.19(1)	0.540(9)	0.99973
4.0	7.55(2)	2.96(5)	0.18(1)	0.485(9)	0.99973
4.2	7.19(2)	2.85(5)	0.17(1)	0.434(8)	0.99971
4.4	6.87(3)	2.85(9)	0.16(2)	0.40(1)	0.99916
4.6	6.58(2)	2.66(6)	0.15(1)	0.347(8)	0.99970
4.8	6.31(2)	2.59(6)	0.14(1)	0.308(8)	0.99969
5.0	6.06(2)	2.50(7)	0.12(1)	0.271(7)	0.99969
5.2	5.83(2)	2.42(7)	0.11(1)	0.236(7)	0.99970
5.4	5.62(2)	2.34(8)	0.10(2)	0.203(7)	0.99972
5.6	5.42(1)	2.23(9)	0.09(2)	0.171(7)	0.99975
5.8	5.24(1)	2.1(1)	0.08(2)	0.141(7)	0.99980
6.0	5.07(1)	1.9(1)	0.08(2)	0.113(7)	0.99984

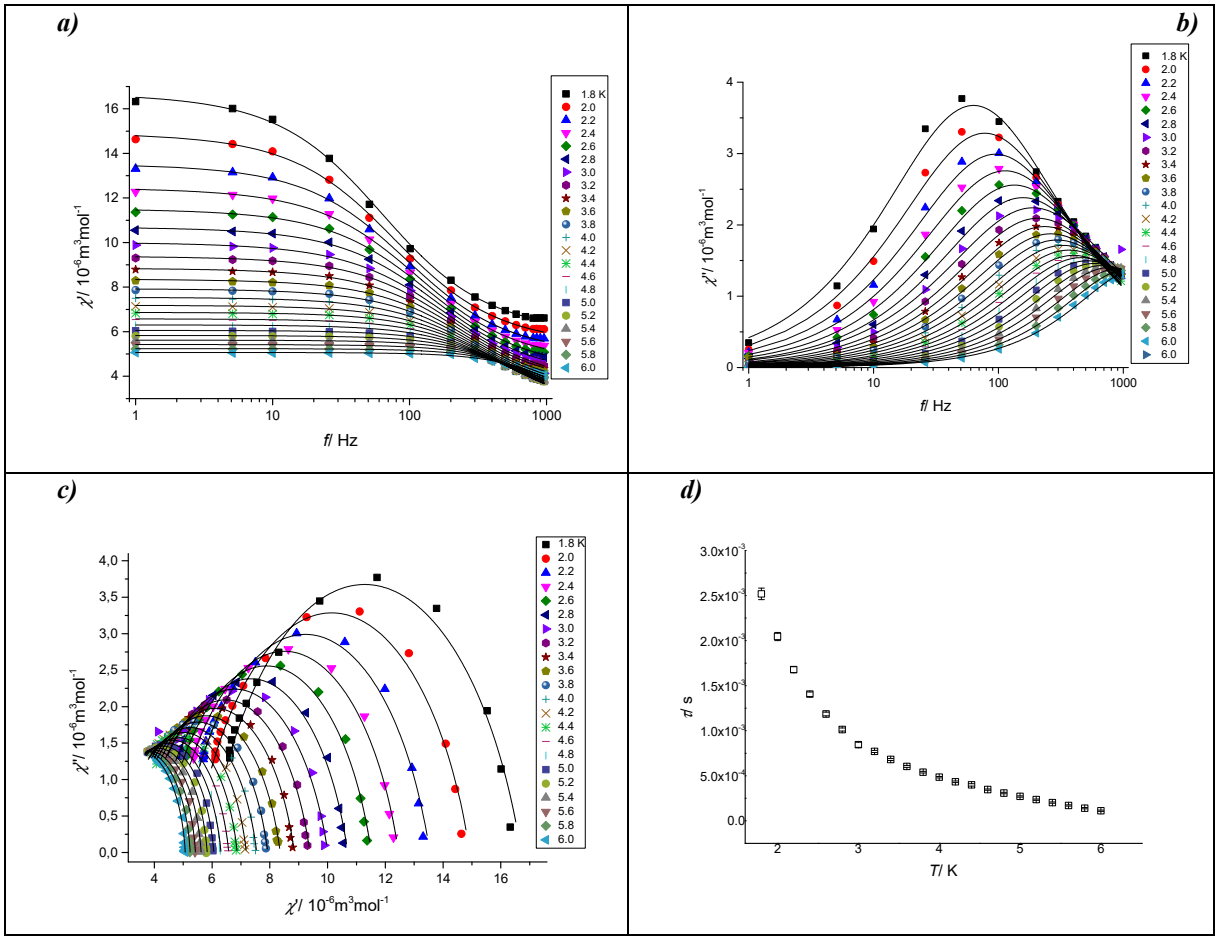

Figure S23 AC susceptibility data for **II** recorded at various temperatures at 1000 Oe: Frequency dependent in-phase χ'(*a*) and out-of-phase χ''(*b*) component of AC susceptibility and Cole-Cole diagram (*c*) (solid lines are results of fits according to equations S1 and S2). Temperature dependency of relaxation time τ with standard errors

Table S16 Parameters of the extended one-set Debye model (eq. S1 and S2) for **II** measured at 0.15 T.

T /K	χ_T /10^{-6} m^3 mol^{-1}	χ_S /10^{-6} m^3 mol^{-1}	α	τ /10^{-3} s	R^2
1.8	81.4(5)	17.9(4)	0.24(1)	2.54(7)	0.99899
2.0	73.1(4)	16.4(3)	0.23(1)	2.11(5)	0.99923
2.2	66.6(3)	15.2(3)	0.228(9)	1.76(3)	0.99939
2.4	61.5(3)	14.2(3)	0.222(9)	1.49(3)	0.99943
2.6	57.1(2)	13.3(3)	0.218(8)	1.27(2)	0.99952
2.8	53.3(2)	12.5(2)	0.216(8)	1.09(2)	0.99958
3.0	49.9(2)	11.8(2)	0.212(8)	0.95(1)	0.99960
3.2	46.9(2)	11.2(2)	0.209(8)	0.83(1)	0.99962
3.4	44.3(1)	10.7(1)	0.207(8)	0.73(1)	0.99965
3.6	42.0(1)	10.2(3)	0.203(9)	0.651(1)	0.99963
3.8	39.8(1)	9.8(3)	0.195(9)	0.58(9)	0.99964
4.0	37.9(1)	9.5(3)	0.188(9)	0.52(8)	0.99963
4.2	36.2(1)	9.2(3)	0.18(1)	0.46(8)	0.99962
4.4	34.6(1)	8.9(3)	0.17(1)	0.42(7)	0.99963
4.6	33.2(1)	8.7(3)	0.16(1)	0.37(7)	0.99962
4.8	31.8(1)	8.4(3)	0.15(1)	0.33(7)	0.99964
5.0	30.62(9)	8.1(3)	0.13(1)	0.29(6)	0.99964
5.2	29.48(9)	7.9(4)	0.12(1)	0.25(6)	0.99968
5.4	28.42(8)	7.5(4)	0.11(1)	0.22(6)	0.99973
5.6	27.43(7)	7.1(4)	0.10(1)	0.18(6)	0.99976
5.8	26.52(6)	6.6(5)	0.10(1)	0.15(5)	0.99982
6.0	25.69(7)	5.2(8)	0.10(2)	0.12(7)	0.99972

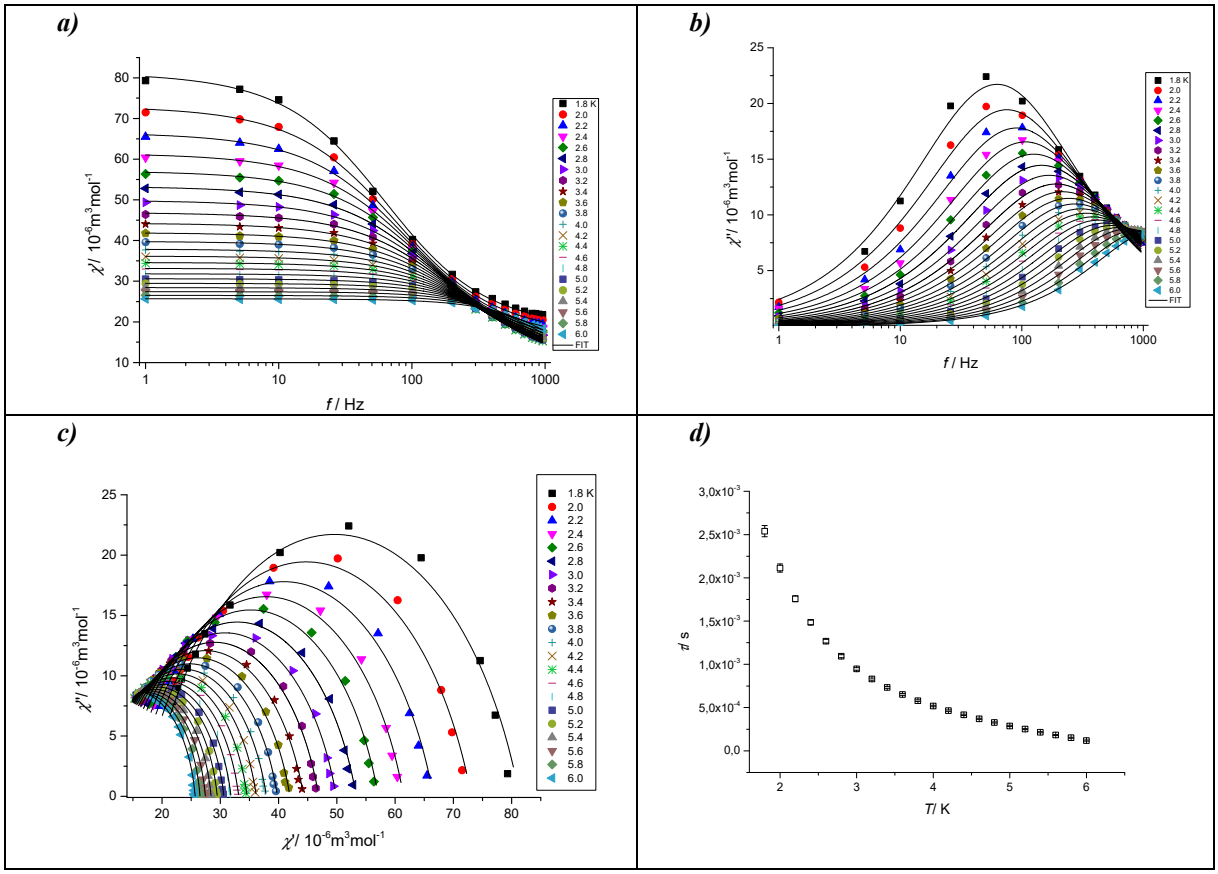

Figure S24 AC susceptibility data for **II** recorded at various temperatures at 0.15 T: Frequency dependent in-phase χ'(*a*) and out-of-phase χ''(*b*) component of AC susceptibility and Cole-Cole diagram (*c*) (solid lines are results of fits according to equations S1 and S2). Temperature dependency of relaxation time τ with standard errors

Table S17 Parameters of the extended one-set Debye model (eq. S1 and S2) for **II** measured at 0.2 T.

T /K	χ_T / 10^{-6} m^3 mol^{-1}	χ_S / 10^{-6} m^3 mol^{-1}	α	τ /10^{-3} s	R^2
1.8	81.4(5)	17.9(4)	0.24(1)	2.54(7)	0.99899
2.0	73.1(4)	16.4(3)	0.23(1)	2.11(5)	0.99923
2.2	66.6(3)	15.2(3)	0.228(9)	1.76(3)	0.99939
2.4	61.5(3)	14.2(3)	0.222(9)	1.49(3)	0.99943
2.6	57.1(2)	13.3(3)	0.218(8)	1.27(2)	0.99953
2.8	53.3(2)	12.5(2)	0.216(8)	1.09(2)	0.99958
3.0	49.9(2)	11.8(2)	0.212(8)	0.94(1)	0.99960
3.2	46.9(2)	11.2(2)	0.209(8)	0.83(1)	0.99962
3.4	44.3(1)	10.7(2)	0.207(8)	0.73(1)	0.99965
3.6	42.0(1)	10.2(2)	0.203(9)	0.65(1)	0.99963
3.8	39.8(1)	9.8(2)	0.195(9)	0.580(9)	0.99964
4.0	37.9(1)	9.5(2)	0.188(9)	0.52(8)	0.99963
4.2	36.2(1)	9.2(3)	0.18(1)	0.465(8)	0.99962
4.4	34.6(1)	8.9(3)	0.17(1)	0.415(7)	0.99963
4.6	33.2(1)	8.7(3)	0.16(1)	0.370(7)	0.99962
4.8	31.8(1)	8.4(3)	0.15(1)	0.328(7)	0.99964
5.0	30.6(1)	8.1(3)	0.14(1)	0.288(6)	0.99964
5.2	29.48(9)	7.9(4)	0.12(1)	0.251(6)	0.99968
5.4	28.42(8)	7.5(4)	0.11(1)	0.215(6)	0.99973
5.6	27.43(7)	7.1(4)	0.10(1)	0.183(6)	0.99976
5.8	26.52(6)	6.6(5)	0.10(1)	0.152(5)	0.99982
6.0	25.69(7)	5.3(8)	0.10(2)	0.119(7)	0.99972

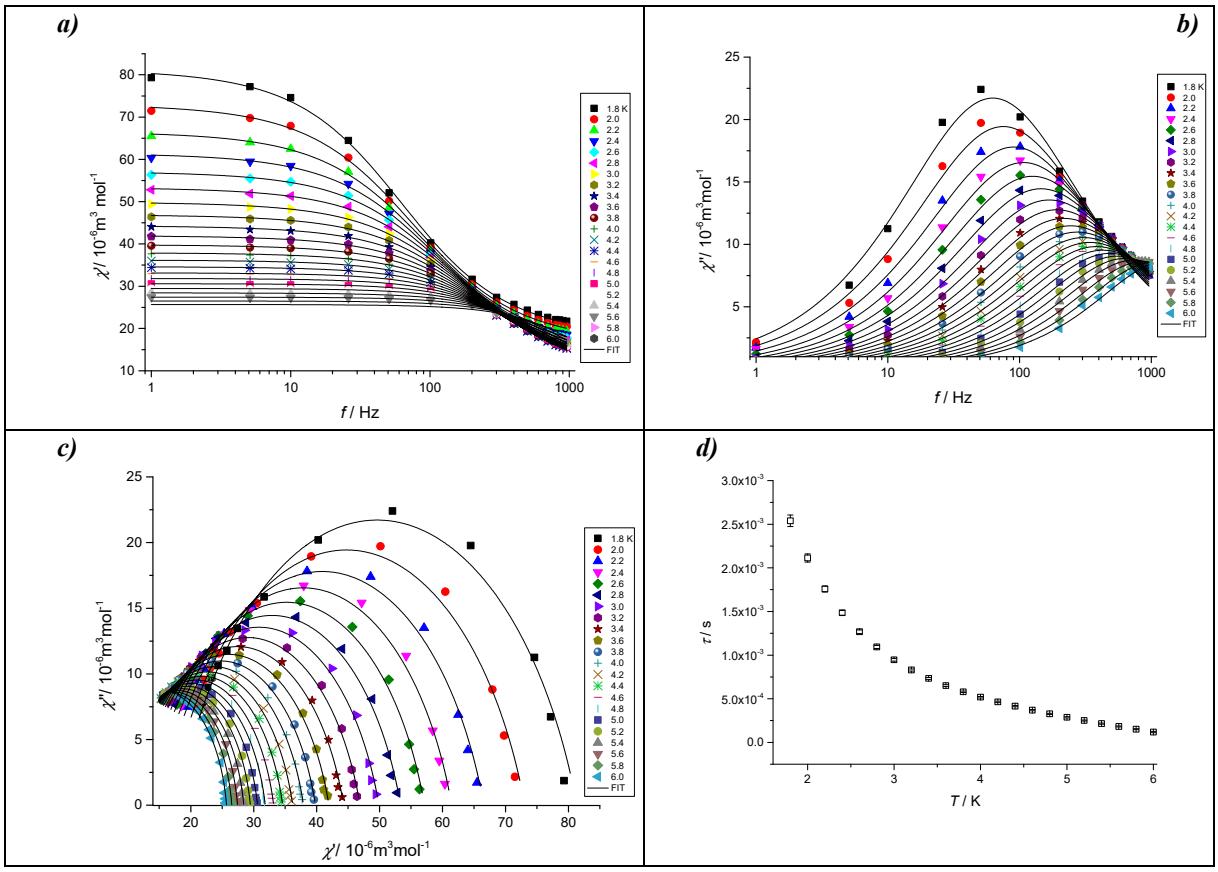

Figure S25 AC susceptibility data for **II** recorded at various temperatures at 0.2 T: Frequency dependent in-phase χ'(*a*) and out-of-phase χ''(*b*) component of AC susceptibility and Cole-Cole diagram (*c*) (solid lines are results of fits according to equations S1 and S2). Temperature dependency of relaxation time τ with standard errors

Table S18 Relaxation parameters for compound **I** using the combination of Raman and direct mechanisms

Model	U/k_B / K	τ_0/s	C / K^{-n} s^{-1}; n	AB^m / T^{-m} K^{-1} s^{-1}	R^2
0.02 T Orbach+Raman*	6.2(3)	$2.6(3)\times10^{-4}$	$3.51(8)\times10^{-4}$; 9	-	0.99882
0.02 T Raman+direct*	-	-	$2.2(3)\times10^{-3}$; 9	368(28)	0.95783
0.02 T Orbach for 4.0 K – 6.4 K	52(2)	$6(2)\times10^{-8}$	-	-	0.98974
0.10 T Orbach+Raman*	7.42(3)	$3.2(3)\times10^{-4}$	$2.53(4)\times10^{-4}$; 9	-	0.99945
0.10 T Raman+direct*	-	-	$2.8(2)\times10^{-4}$; 9	5.7(5)	0.99347
0.10 T Orbach for 4.8 K – 8.0 K	38(2)	$5(2)\times10^{-7}$	-	-	0.97227

*Raman exponent has been fixed to n=9

Table S19 Relaxation parameters at B_{DC} = 0.05 T for compound **II** using the respective combinations of Orbach, Raman and Direct mechanisms.

Model	U/k_B / K	τ_0/s	C / K^{-n} s^{-1}; n	AB^m / T^{-m} K^{-1} s^{-1}	R^2
Orbach+Raman*	4.2(7)	$2.0(5)\times10^{-4}$	0.0021(2); 9	-	0.96897
Orbach+direct	60(9)	$2(3)\times10^{-9}$	-	411(33)	0.95152
Raman+direct*	-	-	0.0022(3); 9	368(28)	0.95783
Orbach+Raman+direct*	4.3(7)	$2.1(5)\times10^{-4}$	0.0021(3); 9	20(0)	0.96886
Orbach for 5.0 K – 6.0 K	65(12)	$5.8(2)\times10^{-10}$	-	-	0.85798

*Raman exponent has been fixed to n=9

Table S20 Relaxation parameters at B_{DC} = 0.1 T for compound **II** using the respective combinations of Orbach. Raman and Direct processes of relaxation.

Model	U/k_B / K	τ_0/s	C / K^{-n} s^{-1}; n	AB^m / T^{-m} K^{-1} s^{-1}	R^2
Orbach+Raman*	5.3(7)	$1.41(5)\times10^{-4}$	6.0(2); 9	-	0.99793
Orbach+direct	19(2)	$8(3)\times10^{-6}$	-	266(17)	0.98391
Raman+direct	-	-	5(2); 3.9(3)	218(20)	0.99162
Orbach+Raman+direct*	7.9(3)	$1.08(5)\times10^{-4}$	$5.1(1)\times10^{-4}$; 9	153(8)	0.99978
Orbach for 5.0 K – 6.0 K	26(2)	$1.6(6)\times10^{-6}$	-	-	0.97412

*Raman exponent has been fixed to n=9

Table S21 Relaxation parameters at B_{DC} = 0.15 T for compound **II** using the respective combinations of Orbach, Raman and Direct processes of relaxation.

Model	U/k_B / K	τ_0/s	C / K^{-n} s^{-1}; n	AB^m / T^{-m} K^{-1} s^{-1}	R^2
Orbach+Raman	4.5(2)	$2.2(2)\times10^{-4}$	0.05(4); 6.5(4)	-	0.99695
Orbach+direct	20(2)	$7(2)\times10^{-6}$	-	259(14)	0.98695
Raman+direct	-	-	3(2); 4.1(3)	220(15)	0.99362
Orbach+Raman+direct	9.9(3)	$7.7(5)\times10^{-5}$	$4(2)\times10^{-5}$; 10.4(3)	190(4)	0.99993
Orbach+Raman+direct*	8.8(3)	$1.02(5)\times10^{-5}$	$4.7(1)\times10^{-4}$; 9	178(5)	0.9998
Orbach for 5.0 K – 6.0 K	26(2)	$1.7(2)\times10^{-6}$	-	-	0.97153

*Raman exponent has been fixed to n=9

Table S22 Relaxation parameters at B_{DC} = 0.20 T for compound **II** using the respective combinations of Orbach, Raman and Direct processes of relaxation.

Model	U/k_B / K	τ_0/s	C / K^{-n} s^{-1}; n	AB^m/ T^{-m} K^{-1} s^{-1}	R^2
Orbach+Raman	4.5(2)	$2.2(2)\times10^{-4}$	0.05(4); 6.5(4)	-	0.99854
Orbach+direct	20(2)	$7(2)\times10^{-6}$	-	259(14)	0.98695
Raman+direct	-	-	3(2); 4.1(3)	220(15)	0.99362
Orbach+Raman+direct	9.9(3)	$7.7(5)\times10^{-5}$	$4(3)\times10^{-5}$; 10.4(3)	190(3)	0.99993
Orbach+Raman+direct*	8.8(3)	$1.02(5)\times10^{-5}$	$4.7(1)\times10^{-4}$; 9	178(5)	0.9998
Orbach for 5.0 K – 6.0 K	26(2)	$1.7(2)\times10^{-6}$	-	-	0.97153

*Raman exponent has been fixed to n=9